UNIVERSITY OF CRETE

SCHOOL OF SCIENCES AND ENGINEERING

DEPARTEMENT OF CHEMISTRY

LABORATORY OF BIOINORGANIC CHEMISTRY

IN COLLABORATION WITH:

INSTITUTE DES SCIENCES MOLECULAIRES DE MARSEILLE (ISM2)

TEAM BIOSCIENCES, AIX – MARSEILLE UNIVERSITY

MARSEILLE, FRANCE

Master of Science Thesis

Design and synthesis of porphyrins and their effect in laccase's activity for the catalysis of dioxygen reduction

Athanasia Petrou

Supervisors: Thierry Tron, Athanassios G. Coutsolelos

Heraklion 2015

ΠΑΝΕΠΙΣΤΗΜΙΟ ΚΡΗΤΗΣ

ΣΧΟΛΗ ΘΕΤΙΚΩΝ ΚΑΙ ΤΕΧΝΟΛΟΓΙΚΩΝ ΣΠΟΥΔΩΝ

ΤΜΗΜΑ ΧΗΜΕΙΑΣ

ΕΡΓΑΣΤΗΡΙΟ ΒΙΟΑΝΟΡΓΑΝΗΣ ΧΗΜΕΙΑΣ

ΣΕ ΣΥΝΕΡΓΑΣΙΑ ΜΕ:

INSTITUTE DES SCIENCES MOLECULAIRES DE MARSEILLE (ISM2)

ΟΜΑΔΑ BIOSCIENCES, ΠΑΝΕΠΙΣΤΗΜΙΟ AIX – MARSEILLE

ΜΑΣΣΑΛΙΑ, ΓΑΛΛΙΑ

Μεταπτυχιακό Δίπλωμα Ειδίκευσης

Σχεδιασμός και σύνθεση πορφυρινών και η επίδρασή τους στην δραστικότητα της λακάσης για καταλυτική αναγωγή οξυγόνου

Αθανασία Πέτρου

Επιβλέποντες Καθηγητές: Thierry Tron, Αθανάσιος Γ. Κουτσολέλος

Ηράκλειο 2015

Committee

Athanassios G. Coutsolelos

Professor of Inorganic Chemistry, Department of Chemistry, University of Crete, Greece

Thierry Tron

Doctor, Institute des Sciences Moleculaires des Marseille (ism2), Biosciences, Marseille, France

Constantinos Milios

Assistant Professor of Inorganic Chemistry, Department of Chemistry, University of Crete, Greece

To my family

Acknowledgements

The present master thesis was carried out in Laboratory of Bioinorganic Chemistry of Chemistry Department in University of Crete under the supervision of Professor Athanassios G. Coutsolelos. I would like to thank him for guidance, encouragement and financial supporting. I feel grateful for giving me the opportunity to work together and the trust he showed.

This master thesis was in collaboration with the Institute des Sciences Moleculaires des Marseille (ism2), Biosciences team in Marseille, France under the supervision of Dr. Thierry Tron. I would also like to thank him for his advice and guidance.

I would like to thank Assistant Professor Constantino Milio, of Chemistry Department in University of Crete, for spending his valuable time on reading this master thesis and for accepting to be member of my committee.

Moreover, I would like to thank Dr. Pierre Rousselot - Pailley from Institute des Sciences Moleculaires des Marseille (ism2), Biosciences for his help. I could not forget Ph. D candidate Marianthi Kafentzi from Biosciences team for her advice and discussions that we had all this time and particularly during my visits in Marseille.

At this point, I would like to thank Professor Dimitrios Ganotakis and all the members of Biochemistry Lab of Chemistry Department in University of Crete, for allowing me to perform the dioxygen consumption measurements.

I owe a big thank to Ph. D George Charalampidis for his advice and time that he spent since I came to the lab to carry out my undergraduate research project until now.

I could not forget all the members of Bioinorganic Lab for their supporting, advice and for such an amazing workplace all these years. I feel so lucky meeting these people and spending such a great time together.

Last but not least, I would like to thank all my friends in Crete and in my hometown for being real friends and I owe the greatest “thank you” to my family for standing by me and giving me encouragement to move on even when I lose my strength.

Abstract

In recent years, great effort has been devoted to the development of new technologies for catalyze reactions using solar energy as a sole source of energy. Several publications have appeared documenting approaches where an association of enzyme (catalyst) and photosensitizer, [1-4] allow performing redox reactions such as O_2 oxidation or H_2 reduction. In addition, a separate area of research, focuses on design of photo-driven systems using photosensitizer and enzyme for catalyzing chemical transformations using water or dioxygen as oxygen atom source [5].

However, there are many factors such as the necessary presence of sacrificial electron acceptor and inert conditions or the production of reactive oxygen species which should be considered. Therefore, the design of a photocatalytic system that could potentially use the atmosphere's dioxygen as the final electron acceptor, in such catalytic systems, is of major importance.

In the present study, we describe the design of hybrid photocatalytic systems consisting of photosensitizers and an enzyme (laccase) co-absorbed on TiO_2 nanoparticles. These systems are designed to catalyze visible - driven oxidation of organic substrates, e.g. an alkene to epoxide, with O_2 as oxidant, under mild conditions, at room temperature.

Porphyrins, corroles and RuP were selected as photosensitizers. The effectiveness of nine different photosensitizers, free base and metallated, bearing phosphonate and carboxylate anchoring groups, linked either directly or through alkyl chains at *p*-position of their peripheral phenyl groups was investigated in this study. Porphyrins, corroles as well as RuP [3] appear of high stability, high absorption in the visible spectrum and having long life time in their excited states. On the other hand, the enzyme laccase belongs to the family of multicopper oxidases which couple the oxidation of a wide range of organic or inorganic compounds with the concomitant reduction of O_2 to water [6].

At first, dioxygen comsumption experiments were performed with all the photosensitizers and the best ratios of both photosensitizer and laccase leading to optimal performance were identified. RuP and porphyrins bearing carboxylate and phosphonate groups at the *p*-position of their peripheral phenyl groups showed the best performance.

Taking into consideration the results of dioxygen consumption measurements, the best performing photosensitizers were also studied for their potential use in the photocatalytic oxidation of *p*-styrene under mild conditions. Unfortunately, none of our system displays photocatalytic activity during visible-light driven oxidation of organic compounds

.

Keywords: porphyrin, RuP, laccase, multi-copper oxidases, dioxygen reduction, TiO_2 nanoparticles, photoreduction, p-styrene, photooxidation

Περίληψη

Τα τελευταία χρόνια, έχει γίνει μεγάλη προσπάθεια στην ανάπτυξη νέων τεχνολογιών στην κατάλυση αντιδράσεων χρησιμοποιώντας την ηλιακή ενέργεια ως τη μόνη πηγή ενέργειας, Σε αρκετές δημοσιεύεις, έχει αναφερθεί ότι ο συνδυασμός ενός ενζύμου (καταλύτη) και ενός φωτοευαισθητοποιητή[1-4] επιτρέπει την πραγματοποίηση οξειδοαναγωγικών αντιδράσεων όπως οξείδωση του μοριακού οξυγόνου ή την αναγωγή του μοριακού υδρογόνου. Ωστόσο, ένα ξεχωριστό κομμάτι έρευνας επικεντρώνεται στο σχεδιασμό φωτο-επαγόμενων συστημάτων χρησιμοποιώντας φωτοευαισθητοποιητή και ένζυμο για την κατάλυση χημικών μετασχηματισμών με τη χρήση νερού ή O_2 ως πηγή οξυγόνου [5].

Όμως, υπάρχουν πολλοί παράγοντες που θα πρέπει να λάβουμε σοβαρά υπόψη μας όπως η απαραίτητη ύπαρξη θυσιαζόμενου δέκτη ηλεκτρονίων και αδρανών συνθηκών και η παραγωγή δραστικών ειδών οξυγόνου.

Στην παρούσα εργασία, περιγράφουμε το σχεδιασμό υβριδικών, φωτοκαταλυτικών συστημάτων αποτελούμενων από φωτοευαισθητοποιητή και λακάση, προσροφημένων πάνω σε νανοσωματίδια TiO_2 nanoparticles, Τα συστήματα αυτά θα έχουν την ικανότητα κατάλυσης φωτο-επαγόμενης οξείδωσης ενός αλκενίου σε εποξείδιο με τη χρήση του O_2 ως οξειδωτικό, κάτω από ήπιες συνθήκες, σε θερμοκρασία δωματίου.

Οι πορφυρίνες, οι κορρόλες και το σύμπλοκο ρουθηνίου επιλέχθηκαν ως φωτοευαισθητοποιητές. Μελετήθηκε η αποτελεσματικότητα εννέα διαφορετικών φωτοευαισθητοποιητών, μεταλλωμένων και μη, που φέρουν φωσφορικές και καρβοξυλικές ομάδες πρόσδεσης στις *πάρα*- θέσεις των περιφερειακών φαινυλίων, συνδεδεμένες είτε απευθείας είτε μέσω ανθρακικών αλυσίδων. Τόσο οι πορφυρίνες και οι κορρόλες, όσο και τα σύμπλοκα του ρουθηνίου[3] εμφανίζουν μεγάλη σταθερότητα, υψηλή απορρόφηση στο φάσμα ορατού και μεγάλο χρόνο ζωής των διεγερμένων καταστάσεων. Από την άλλη πλευρά, το ένζυμο λακάση ανήκει στην οικογένεια πολυ-πυρηνικών οξειδασών χαλκού, που φέρουν πολλά μεταλλικά κέντρα χαλκού, που μπορούν να συνδυάσουν την οξείδωση μεγάλης ποικιλίας οργανικών και ανόργανων υποστρωμάτων [6] με ταυτόχρονη αναγωγή του μοριακού οξυγόνου σε νερό.

Αρχικά, πραγματοποιήθηκαν μετρήσεις κατανάλωσης οξυγόνου με όλους τους φωτοευαισθητοποιητές και προσδιορίστηκαν οι βέλτιστες αναλογίες

φωτοευαισθητοποιητή και λακάσης για τη βέλτιστη κατανάλωση. Το σύμπλοκο ρουθηνίου και οι πορφυρίνες που φέρουν καρβοξυλικές και φωσφορικές ομάδες άμεσα συνδεδεμένες στην πάρα- θέση των περιφερειακών φαινυλίων έδειξαν τα καλύτερα αποτελέσματα.

Λαμβάνοντας υπόψη τα αποτελέσματα των μετρήσεων κατανάλωσης οξυγόνου, οι φωτοευαισθητοποιητές με τις βέλτιστες τιμές κατανάλωσης μελετήθηκαν και ως προς τη χρήση τους για φωτο-επαγόμενη οξείδωση p-στυρενίου χωρίς την προσθήκη θυσιαζόμενου δότη ηλεκτρονίων. Ωστόσο, κανένα από τα συστήματα που μελετήσαμε δεν παρουσίασε φωτοκαταλυτική δράση κατά την φωτο-επαγόμενη οξείδωση οργανικών ενώσεων.

Λέξεις-κλειδιά: πορφυρίνη, σύμπλοκο ρουθηνίου, λακάση, πολύ-πυρηνικές οξειδάσες χαλκού, αναγωγή μοριακού οξυγόνου, νανοσωματίδια TiO_2, φωτοαναγωγή, p-στυρένιο, φωτοοξείδωση.

Table of Contents

Chapter 1 – Introduction

1. Laccases

Laccase (p-diphenol: oxygen oxidoreductase,) representing the largest subgroup of blue multicopper oxidases (MCO), is a copper-containing oxidase that catalyzes reduction of molecular oxygen to water. Amongst more than 200 kinds of oxidases and oxygenases, only six classes of enzymes are capable of catalyzing this type of oxygen reaction (cytochrome-c oxidase, laccases, L-ascorbate oxidase, ceruloplasmin, bilirubin oxidase, and phenoxazinone synthase).

Laccases are also very interesting because of their structure and catalytic mechanisms. The laccase active site contains four copper ions of three types the coordinated interaction of which during catalysis couples the one-electron oxidation of substrates to the four-electron reduction of molecular oxygen to water. The substrate specificity of laccases is also very attractive because of their ability to catalyze the oxidation [7] of a wide range of organic and inorganic substrates including mono-, di-, and polyphenols [8], amino phenols, methoxy phenols, aromatic amines and ascorbate with the concomitant reduction of molecular oxygen to water [9](see **Figure 1.1**).

Figure 1: Schematic representation of laccase-catalyzed oxidation redox cycles for substrates oxidation.

1.1. Distribution in nature

Laccase was first isolated from sap of the lacquer tree *Rhus vernicifera* late in the 19th century. Since then, laccases have also been found in various basidiomycetE and ascomycete fungi and fungal laccases have accounted for the most important group of MCOs with respect to number and extent of characterization [10].

In fungi, laccases carry out a variety of physiological roles including morphogenesis, fungal plant pathogen/host interaction, stress defense, and lignin degradation [6]. Moreover, laccases are the most important components of the lignolytic arsenal of wood-destroying white rot fungi but its role in these processes is not known in detail.

Although, laccases are widely distributed in plants and fungi, laccase activity has been reported in only few bacteria. In this case, laccases appear to have a role in morphogenesis, in the biosynthesis of the brown spore pigment and in the protection afforded by the spore coat against UV light and hydrogen peroxide.

In insects, the main function of the laccase-type proteins is believed to be sclerotization of the cuticle in the epidermis.

1.2. Structure of the active site of laccase

The active site of laccase contains four copper ions: a mononuclear “blue” copper ion (T1 site) and a three nuclear copper cluster (T2/T3 site) consisting of one T2 copper ion and two T3 copper ions [11-15]. The type 2 and type 3 play a key role in the reduction of dioxygen to water. The T1 copper site of laccases, responsible for the oxidation of substrates, is located near the enzyme’s surface in the third domain (D3), and the three-nuclear cluster T2/T3 is located between the first (D1) and third (D3) domains and has amino acid ligands in each of them (see **Figure 2**). Amino acid residues of the second and third domains are involved in the formation of the substrate-binding pocket (the binding site of electron donor substrate). The distance between the T2 and T3 sites of the enzyme is 4 Å and the T1 copper ion is located at the distance of about 12 Å from them.

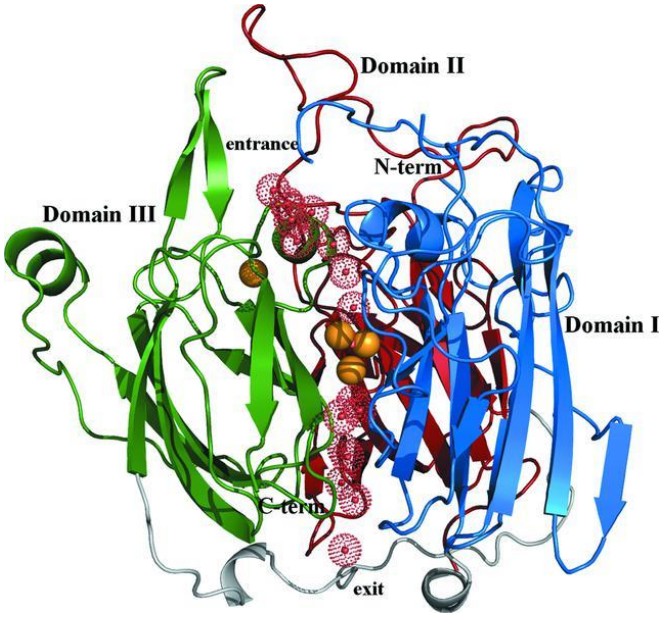

Figure 2: Three-dimensional structure of CotA laccase: overall three-dimensional fold highlighting the entrance and exit channels, above and below the trinuclear cluster, for the dioxygen and water molecules, respectively. The three cupredoxin-like domains are coloured blue (domain 1), dark red (domain 2) and green (domain 3). Cu atoms are represented as spheres coloured yellow.

Copper ions of the laccase active site are classified on the basis of their spectroscopic characteristics (electronic absorption and EPR). The T1 Cu site of laccases offers a light blue color to the enzyme solutions and is characterized by a distinctly noticeable band of optic absorption at the wavelength of 610 nm (e ~ 5600M^{-1}·cm^{-1}) and also by a weak parallel superfine splitting in the EPR spectra. The T1 Cu is coordinated to the nitrogens of imidazoles from two histidines through strong covalent π bond and the sulfhydryl group of cysteine, which form a trigonal structure, (see **Figure 3)**. The π-covalent bond between T1 copper and sulphur atom is responsible for the blue colour (LMCT) [13, 15]. In some cases of multi-copper proteins, a methionine ligand occupies the fourth coordination site, whereas in others there is an uncoordinated ligand, leucine or phenylalanine.

The mononuclear T2 site of the enzyme, which is invisible in electron absorption spectra, displays ultrafine splitting in EPR spectra which is typical for copper ions in tetragonal complexes. Type 2 copper is coordinated to the nitrogens of imidazoles from two histidines and one water molecule through oxygen atom. The T2 site can be selectively removed from the enzyme molecule, and this is accompanied by a significant loss in the enzyme activity [10].

The T3 site of laccases is a binuclear copper site with copper ions paired antiferromagnetically through a hydroxide bridge that makes this site diamagnetic and prevents its detection in the EPR spectra. This site can be identified by the presence of a shoulder at 330 nm (e ~ 5000M^{-1}·cm^{-1}) in the UV region of the spectrum. Each T3 Cu ion is coordinated to three imidazoles of histidines and one hydroxyl bridging group as mentioned above.

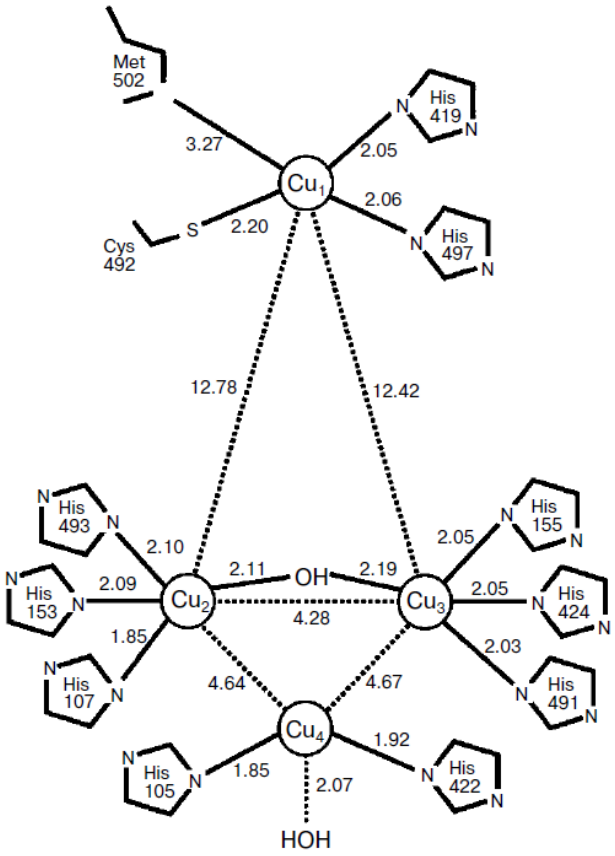

Figure 3: Presentation of T1 (Cu1) and T2/T3 (Cu4/ Cu2 Cu3) copper sites of laccase CotA from *Bacillus Subtilis*.

1.3. O_2 Reduction

In spite of many works concerning blue copper-containing oxidases including laccases, there is no general opinion about the electron transfer pathway inside the protein and namely the mechanism [12,15,16] of dioxygen reduction in the molecule.

Electrons are transferred from substrate molecules through the type 1 copper ion to the trinuclear centre. Dioxygen binds to the trinuclear centre and after the transfer of four electrons is reduced to two molecules of water. Both entrance and exit channels contain residues such as aspartate and glutamate that can serve as providers of protons.

Despite extensive studies over the past decade, the exact mechanism of dioxygen reduction remains one of the outstanding questions to be answered. A considerable amount of spectroscopic and kinetics work has been focused on laccases such as *Rhus vernicifera* [17], and more recently on the laccase-like, Fet3p protein from *Saccharomyces cerevisiae* [18].

Recent X-ray structural studies on the CotA enzyme [19] have not only defined the structure of the peroxide, but in conjunction with other X-ray structural studies on the multi-copper oxidase family, suggest an alternative mechanism for the dioxygen reduction. Initially, dioxygen moves to the trinuclear copper site through a channel which is occupied with solvent molecules. Structural studies on the laccase from CotA indicates that the dioxygen will diffuse to an almost symmetrical binding site within the trinuclear cluster (**Fig.4a**). All the copper oxygen distances lie in the range 2.2–2.6 Å. All the copper ions, in this structure, will be in the oxidized +2 state.

Then, two electrons are transferred to dioxygen and the diatomic O_2^{2-} moiety becomes inclined to the line between Cu2 and Cu3, so the closest Cu–O distances are 1.95 Å (Cu3) and 2.01 Å (Cu2). The pathway of electron transfer in CotA involves substrate molecules donating electrons to the type 1 copper ion through His497 and then the transmission of these electrons through Cys492 and the adjacent histidines, His491 and His493, to Cu3 and Cu2, respectively. Each of the type 3 copper ions can then transfers one electron to an oxygen atom of the bound dioxygen (**Fig. 4b**). After that, the type 3 copper ions will be still in the oxidized +2 state.

The O_2^{2-} moiety may also become protonated at this stage with H^+ being provided by the acidic residues, such as Glu498, in the entrance channel. Two further electrons are then assimilated in a similar manner and cause the peroxide moiety to split into two hydroxyl groups. One of the hydroxyl group remains in a bridging position between the two type 3 copper ions (**Fig. 4c**). The second hydroxyl moiety migrates to the opposite side of the type 2 copper and forms a Cu–OH bond. The migration of the hydroxyl group must involve a

movement of the type 2 copper ion, Cu4, and some transient local distortion of the protein geometry.

The following stages involve the addition of a proton, provided by acidic residues in the exit channel, to the hydroxyl group bound to Cu4 and the release of the first water molecule into the outlet channel. This will leave a structure with only a single hydroxyl moiety bridging the two type 3 copper ions (**Fig. 4d**). This hydroxyl moiety will then migrate to the far side of Cu4, become protonated and finally released as the second water molecule. The enzyme can then bind a second dioxygen molecule for a reiteration of the cycle. Alternatively, in the absence of dioxygen the assimilation of four electrons will leave the enzyme in the fully reduced state (**Fig. 4e**).

From the above, it is evidence that the role of the type 2 copper is twofold; firstly it helps to anchor the dioxygen molecule to the trinuclear cluster prior to reduction and secondly it temporarily binds the hydroxyl groups arising from the reduction of the dioxygen molecule prior to these moieties being released as water molecules into the outlet channel. On the other hand, the type 3 copper ions serve to transfer electrons to the bound dioxygen so that it can be reduced. The mechanism proposed also suggests the reason why there is a separate electron transfer path between the type 1 copper ion and each of the type 3 copper ions, since each of the type 3 copper ions has to give electrons to the bound oxygen.

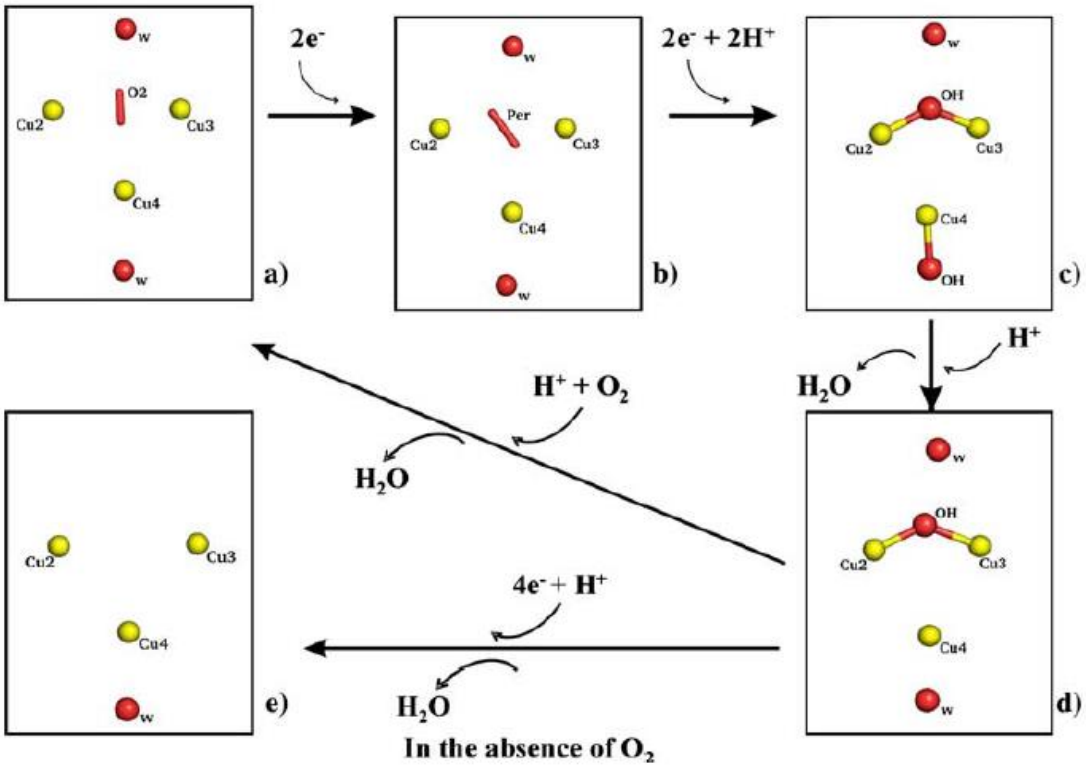

Figure 4: A putative mechanism for the reduction of dioxygen by multi-copper oxidases. a)The ''resting'' state for CotA with a dioxygen molecule bound almost symmetrically between the type 3 copper ions and interacting with the type 2 copper. b) The peroxide intermediate for the CotA enzyme. c) The ''resting'' state where one hydroxyl group bridging the type 3 copper ions and a second attached to the type 2 copper ion at the entrance to the egress channel. d) The molecule with one bridging hydroxyl group as observed in the enzyme from Trametes versicolor. e) The enzyme in its fully reduced state. In neither a nor b is there a hydroxyl group attached to the type 2 copper ion.

1.4. Inhibitors of laccase

The activity of laccases can be inhibited by various organic and inorganic compounds. Compounds like dithiothreitol, thioglycolic and ethyldithiocarbamic acids [20] are described as inhibitors of laccases. In addition, small inorganic anions, such as fluoride [21-23], chloride, azide, and hydroxide anions [13, 15] are able to bind to the T2/T3 site of laccases and prevent the electron transfer from the T1 site of the enzyme into the T2/T3 cluster. In our study, we used sodium fluoride as inhibitor.

In the presene of azide moiety [19], one nitrogen atom (N1) bridges the type 3 copper ions and replacing the oxygen atom of the dioxygen. The N1–Cu2 and N1–Cu3 distances are 2.37 and 2.19 Å, respectively.

The other terminal atom of the azide group, N3, is in precisely the same position as hydroxyl or water molecule and distant by. The presence of azide will inhibit the binding of oxygen to the trinuclear cluster and therefore in addition the activity of the enzyme.

The binding of azide in the CotA enzyme is different from that reported for ascorbate oxidase and ceruloplasmin. In ascorbate oxidase two azide moieties were found to be terminally bound to only one of the type 3 copper ions, whereas for ceruloplasmin only one of these azide moieties was found to bind.

One unusual feature in the azide structure occurs in the vicinity of the mononuclear copper site. There is evidence that the cysteine normally bound to this copper can adopt two positions. In the second position the sulfur atom moves away from the copper and points directly at the terminal methyl group of the adjacent methionine to form a sulfur–carbon bond.

1.5. Factors determining redox potential of the laccase

Standard redox potentials of three copper sites of laccases (T1, T2, T3) are key characteristics of copper containing oxidases including laccases. Based on the T1 site redox potential, all copper containing oxidases are divided onto high, medium, and low potential enzymes [22, 24]. The redox potential of T1 site is known for most laccases as well as the redox potential of T2 site of laccases such as the plant laccase from *R. vernicifera* and fungal laccase from *T. hirsuta* and the T3 site potential is determined for laccases from *R. vernicifera* and *T. versicolor* .

The ligand environment of the T1 copper ion and also the amino acids residues (2^{nd} coordination sphere), play an important role in the redox potential of the three copper sites of laccases. Furthermore, the addition of inhibitors like azide or fluoride ions affect in different way the redox potential of the three coppers sites. The response to any change of the environment or the addition of inhibitors depends on the origin of lacccase.

For example, fluoride ion has a strong influence on redox potential of the T3 site copper ion and slightly affects the potential of copper ions of the T1 and T2 sites [137_143]. In the presence of fluoride ion the potential of the T3 site of laccase from *T. versicolor* is 210 mV lower because of a strong interaction of fluoride ion with the T2/T3 cluster[21].

High potential laccases have a phenylalanine residue as an axial ligand of the T1 site copper; in medium and low potential laccases this role is played by leucine and methionine residue, respectively. The substitution of leucine by phenylalanine in the axial ligand position in laccases from *M. thermophila* and *R. solani* had a slight influence on the T1 site potential and kinetics of substrate oxidation

Moreover, it was recently suggested that an increase in the length of the Cu–N bond should affect the T1 site redox potential because of a decreased contribution of the free electron pair of the nitrogen atom [25]. Comparison of available amino acid sequences of laccases and their redox potentials seems to confirm this hypothesis: laccases which contain glutamic acid and serine in positions corresponding to Glu460 and Ser113 in laccase from *T. versicolor* are high potential. [22, 25]

The range of compounds oxidized by laccases can be enlarged using molecules so-called redox mediators, which are laccase substrates producing high-potential intermediates as a result of enzymatic oxidation. These intermediates can react with other compounds, which cannot be oxidized with the involvement of only laccases. The oxidized mediator is reduced to the initial state by the compound subjected to oxidation, and thus a closed cycle is created [6].

1.6. Influence of pH on laccase activity and stability

The optimum pH for the majority of fungal laccases is in the range from 3.5 to 5.0 and the pH dependence curve is bell shaped [13]. Such a profile of the laccase activity on oxidation of phenolic compounds is caused by two effects. On one hand, with increase in pH of the solution, ionization potential of phenolic compounds decreases. On the other hand, with increase in pH of the solution the rate of laccase catalyzed enzymatic reactions decreases at the cost of OH^- ion binding the T2/T3 site of the enzyme.

The pH optimum of laccase from lacquer tree for substrates that are donors of hydrogen atoms was different from that of fungal laccases: laccase from *Rhus vernicifera* displayed maximal activity in neutral and weakly alkaline solutions. For electron donor substrates, the pH profile of the activity was similar to that of fungal laccases [26].

1.7. Influence of temperature on laccase activity and stability

The temperature optimum of the majority of enzymes is in the limits of 50-70 ^oC, however the activity of laccase from *Ganoderma lucidum* is maximal at 25 ^oC [6,13,27]. Laccases isolated from a strain of *Marasmius quercophilus* have been found to be stable for 1 h at 60 ^oC, while a laccase from *Pleurotus ostreatus* is almost fully active in the temperature range of 40 - 60 ^oC, with maximum activity at 50 ^oC. Another example, a laccase isolated from *G. lucidum* has shown an optimum temperature of 20-25 ^oC and has been found to be stable between 10-50 ^oC for 4 hours. Our laccase, from the fungus *Trametes* sp. C30, has been found stable at 30–40 ^oC for at least 24 hours, but rapidly loses activity at temperatures above 50 ^oC

2. Porphyrins

The porphyrins are an important class of naturally macrocyclic compounds found in biological compounds that play a very important role in the metabolism of living organisms[28, 29]. They have a universal biological distribution and were involved in the oldest metabolic phenomena on earth[30].

The best example is probably protoporphyrin IX. In haeme centers of haemoglobin and myoglobin, it binds iron which can reversibly bind dioxygen in order to transfer it to the cells. The knowledge of these systems and their excited states is essential in understanding a wide variety of biological processes, including oxygen binding, electron transfer[31], catalysis [32, 33], and the initial photochemical step in photosynthesis [34-36]. Without porphyrins and their relative compounds, life as we know it would be impossible.

2.1. The chemical characteristics of porphyrins

The word porphyrin is derived from the Greek *porphura* meaning purple. The porphyrin molecule is a heterocyclic aromatic macrocycle ring and consists of four pyrrole rings linked by four methine bridges. Its structure [37] supports a highly stable configuration of single and double bonds with aromatic characteristics that permit the electrophilic substitution reactions typical of aromatic compounds such as halogenation, nitration, sulphonation, acylation and formylation. There are two different sites on the macrocycle where electrophylic substitution can take place with different reactivity: positions 5, 10, 15, 20, called *meso* and positions 2, 3, 7, 8, 12, 13, 17 and 18, called *β-pyrrole* positions (see **Figure 5**).

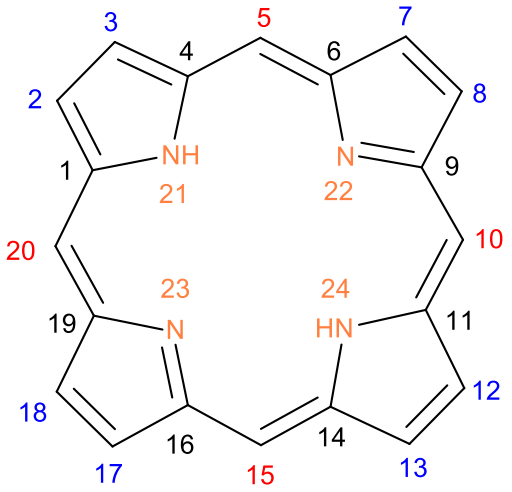

Figure 5: skeleton and numbering of carbons of the porphyrin.

Porphyrins are aromatic compounds that obey the Hückel rule (4n + 2). They have 18π electrons which are delocalized over the entire circumference of the porphyrin ring. Consequently, because of their high conjugation, porphyrins and their derivatives absorb in the visible region which gives their red colour. Generally porphyrins participate in electrophilic and radical reactions due to the aromatic nature of the porphyrin ring. The *meso* positions have a greater electron density, so it is more active. If the *meso* positions are occupied, beta positions can also participate in electrophilic reactions.

The stability of the ring that can be adopted different geometric conformations (**Figure 6**). All atoms of nitrogen of the porphyrin ring have sp^2 hybridization, so all the bond lengths range from 134 -145 pm and angles from 107^o - 126^o. Each sp^2 orbital has an electron able to form π bond with two atoms of carbon and one hydrogen atom. The lone pair of electrons occupying the p-orbital (1) of nitrogen atom, which is perpendicular to the porphyrin ring, offers two electrons in the conjugated system. The atoms of nitrogen which are not bonded with the p-orbital (4) of hydrogen are sp^2 hybridized and offer a lone pair of electrons to assembly with a metal. The p-orbital (3) offers an electron to form π bond with the adjacent atom of carbon (**Figure 7**).

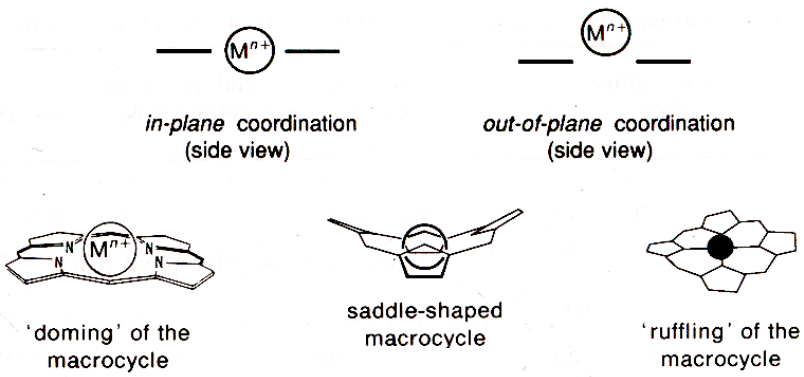

Figure 6: Typical geometric configurations of tetrapyrrolic complexes

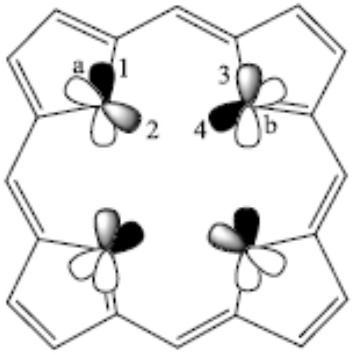

Figure 7: Porphyrin ring

Moreover, porphyrins are unsaturated tetra dented macrocyclic ligands which can bind divalent metal ions that behave as Lewis acids (**Figure 8**). The introduction of metal ions is an easy process including the departure of the two protons inside the macrocyclic core. The size of the porphyrin-macrocycle is perfectly suited to bind almost all metal ions and indeed a large number of metals can be inserted in the center of the macrocycle forming metalloporphyrins that play key roles in several biochemical processes as it is mentioned above.

Figure 8: Reaction of porphyrin's metallation.

2.2. Uv-vis spectra of porphyrins

It was recognized early that the intensity and colour of porphyrins are derived from the highly conjugated π-electron systems and the most fascinating feature of porphyrins is their characteristic UV-visible spectra [37] that consist of two distinct regions: in the near ultraviolet and in the visible region.

As to their electronic absorption, they display extreme intense bands, the so-called *Soret* or *B-bands* in the 380–500 nm range with molar extinction coefficients of 10^5 M^{-1} cm^{-1}. This band corresponds to the transition from the ground state to the second excited state (S0 → S2). Moreover, the second region consists of a weak transition to the first excited state (S0 → S1) in the range between 500-750 nm the so-called *Q bands* with molar extinction coefficients of 10^4 M^{-1} cm^{-1}.

While variations of the peripheral substituents on the porphyrin ring often cause minor changes to the intensity and wavelength of the absorption features, protonation of two of the inner nitrogen atoms or the insertion/change of metal atoms into the macrocycle usually strongly change the visible absorption spectrum. When porphyrin macrocycle is protonated or coordinated with any metal, there is a more symmetrical situation than in the porphyrin free base and this produces a simplification of Q bands pattern for the formation of two Q bands.

2.3. Substituted porphyrins bearing anchoring groups

As we mentioned at the beginning of this chapter, derivatives of porphyrins are found in many biological systems and have a key role in processes like catalysis, electron transfer and oxygen binding. In nature, that kind of processes take place for example in photosynthesis where the solar energy is used to photo-oxidize water into dioxygen.

Recently, several systems associating a photosensitizer and an enzyme, light absorption triggers electron transfer events that lead to the activation of the enzyme's catalytic center have been described. For example, a robust laccase – porphyrin system able to carry out visible light–driven dioxygen reduction has been reported [4]. In another example, the activity of a hydrogenase is driven by light *via* a poly pyridyl complex acting as PS and both the enzyme and the PS are absorbed on TiO_2 nanoparticles. Here, the TiO_2 particles serve

The presence of an anchoring group [38] is essential to graft the photosensitizer into the TiO_2 surface, in order to achieve fast electron injection into the conduction band of TiO_2. Therefore, different porphyrin anchoring groups able to interact with the TiO_2 surface have been presented in the literature. Carboxylate, phosphonate, cyanoacrylate, sulfonate and pyridyl groups are the most commonly used (see **Table 1**).

Anchoring Groups	
Carboxylic acid	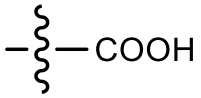
Phosphonic acid	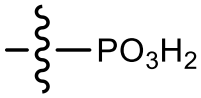
Cyanoacrylic acid	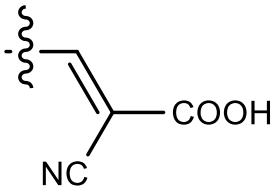
Sulfonic acid	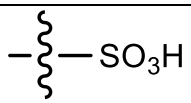
Pyridyl	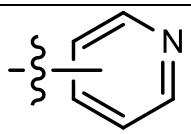

Table 1: Most commonly used anchoring groups.

Carboxylate functional groups serve as grafting agents for the oxide surface of TiO_2 nanoparticles. A carboxylate group can be coordinated to the TiO_2 surface in number of ways: as a unidentate mode, as a chelating mode, and as brindging bidentate mode (**Figure 9**). The unidentate coordination of the carboxylate group results in an ester type bond formation between the carboxylic acid group and the TiO_2 surface. For carboxylate groups, bidentate connections have been shown to be the preferred binding mode on TiO_2

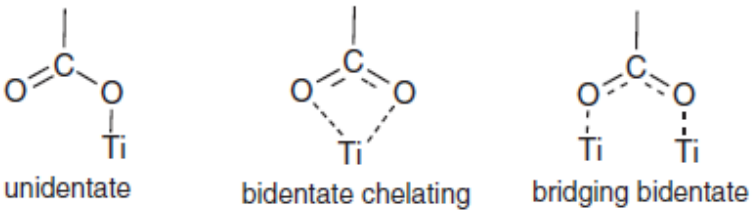

Figure 9: Main binding modes of the carboxylate group to TiO_2.

Phosphonate functional group are used as alternative anchoring groups. Phosphonate has been found more stable and effective than carboxylate. This could be attributed to the intrinsically stronger binding capability of the phosphonate group compared to the carboxylate linkage due to the presence of a hydrogen bond between the atom of phosphorus and the TiO_2. For phosphonate, there were evidences for both bi- and tri-dentate linkages (**Figure 10**), with bi-dentate theoretically determined to be the most stable on crystalline TiO_2 lattices.

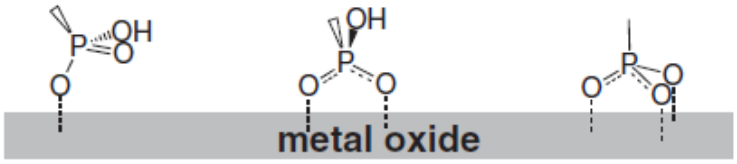

Figure 10: Different binding modes of phosphonates on TiO_2.

Several porphyrins and ruthenium complexes containing anchoring groups such as carboxylic acid, phosphonic acid have been used widely as photosensitizers in photocatalytic systems efficiently. In combination with natural catalysts like enzymes, these systems try to mimick nature and its natural processes i.e photosynthesis in order to find alternative ways to produce renewable hydrogen[3, 39], convert greenhouse gases into organic molecules [2] efficiently and cleanly or carry out chemical transformation [39, 40] using solar energy.

Aim of project

In the last years, scientists have been interested in the development of new synthetic systems catalytically active for reactions like hydrogen oxidation, dioxygen reduction or water splitting to molecular O_2 and H_2. Although some successes have been obtained with such systems, they all so far have a main drawback: in order to keep their catalytic activity, chemical molecules acting as sacrificial electron donors or electron acceptors are required. Thus, the function of these systems relies on the concentration of the electron donor or electron acceptor and also on their life time. That means that, the design of new hybrid catalytic systems containing renewable electron donors or acceptors is of prime importance.

In nature, such processes take place in the absence of sacrificial electron donors or electron acceptors (e. g photosynthesis). Photosynthesis is a complex procedure taking place in plants where the sunlight is the source of energy triggering the decomposition of water into molecular O_2 and H_2 . based on the equation below - through a process of multi electron transfer.

$$\mathbf{2H_2O \rightarrow 2H_2 + O_2}$$

Mimicking the photosynthesis, our goal is to develop stable systems powered by sunlight associating an electron donor to a unit capable to react with dioxygen. One hand photosensitizers are possible candidates as electron shuttle since they are capable of harvesting solar energy. On the other hand, metalloenzymes like laccase act as “oxygen catalytic units”.

Therefore, the aim of this study is the design and development of new hybrid photocatalytic systems type of photosensitizer/laccase absorbed on the surface of a mediator (TiO_2) for dioxygen reduction. Here, we describe the design of hybrid systems photosensitizer/laccase attached to TiO_2 nanoparticles, using different photosensitizers bearing appropriate anchoring groups able to bind to the TiO_2 surface (Scheme 1). We also present the optimal conditions for having the maximum dioxygen consumption for each system.

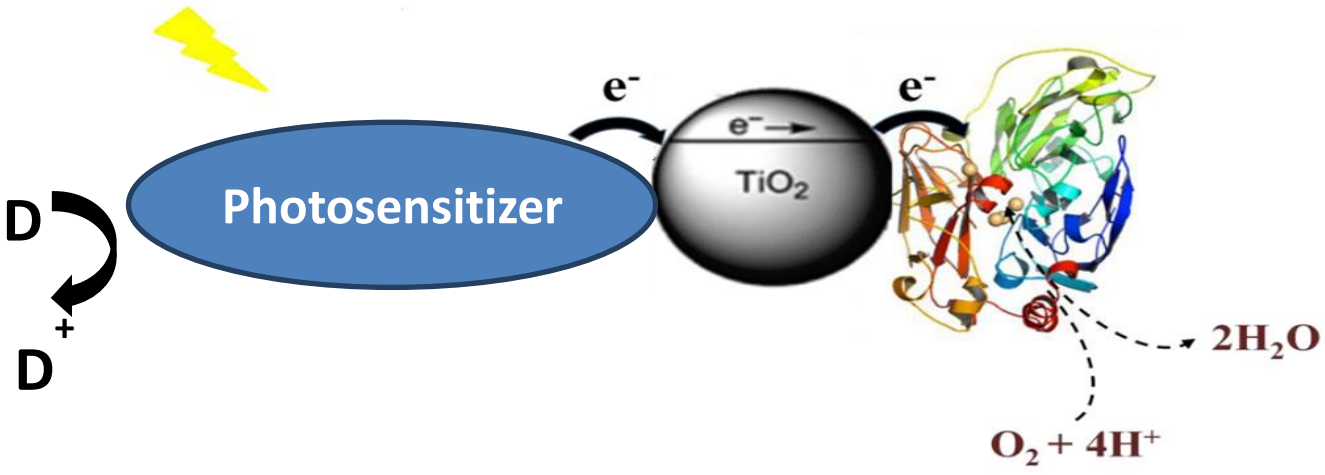

Scheme 1: Dioxygen reduction representation where photosensitizer and laccase are absorbed on TiO_2 nanoparticles.

As already mentioned, the development of robust systems containing photosensitizers and metlloenzymes can support visible light-driven reactions like reduction of molecules such as CO_2 or oxidation of alkene-containing substrates. However, the reactants and the conditions of such reactions are an obstacle to the development of sustainable processes. For this reason, researchers have already studied alternative ways. A photocatalytic system has been recently reported that consists of $[Ru(bpy)_3]^{+2}$/laccase able to oxidize olefins coupled to the light driven reduction of O_2. It is proven that the dioxygen acts as a final and renewable electron acceptor and as the oxygen atom donor. In our work, we studied our photosensitizer/TiO_2/ laccase systems expecting better results as the electron transfer is more efficient (**Scheme 2**)

.

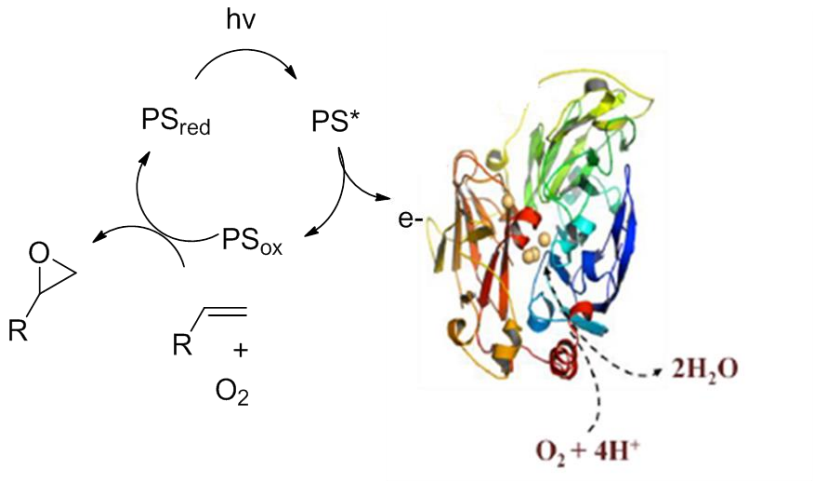

Scheme 2: The photocatalytic system photosesitizer/laccase for epoxidation.

Chapter 2 - Experimental Section

Synthesis of Photosensitizers

Synthesis of 5,10,15,20-tetrakis-(4-carboxyl–methyl-phenyl) porphyrin (1)

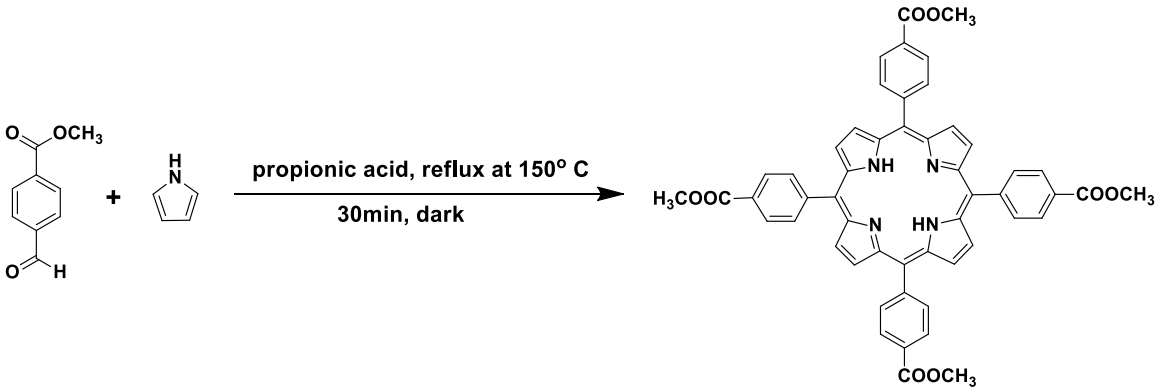

(1)

A solution of methyl-p-formylbenzoate (3.3 g, 20.1 mmol) and pyrrole (1.5 mL, 21.6 mol) in propionic acid (75 mL) was refluxed at 150 ^{o}C in a flask protected from light for 30 min. As soon as the mixture cooled to room temperature, the mixture was washed with distilled water, cold MeOH and Et_2O. The crude product was purified by silica column chromatography eluting with CH_2Cl_2 – EtOH (98:2 v/v). Yield: 733 mg (4.3%).

UV/Vis (CH_2Cl_2): *λmax*: 419, 514, 550, 590, 645 HRMS (MALDI-TOF): m/z calcd. for $C_{52}H_{38}N_4O_8$ [M] 846.27, found 846.45

Synthesis of 5,10,15,20-tetrakis-(4-carboxy–phenyl) porphyrin (2)

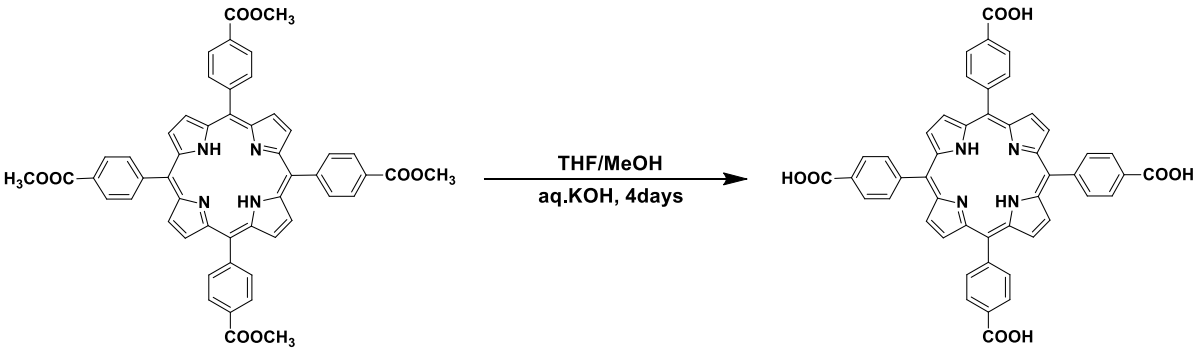

(1) (2)

In a 250 mL round bottom flask, a solution of porphyrin (1) (200 mg, 0.24 mmol) was in THF (70 mL) and MeOH (30 mL) was mixed with a solution of KOH (2 gr, 35.64 mmol) in distilled water (36 mL). The reaction mixture was stirred at room temperature for 4 days. The solvents, THF and MeOH, were completely removed on a rotary evaporator. The rest of the mixture was acidized with HCl 1 M (pH 5). The precipitate was filtered and washed with distilled water many times. Yield: 126 mg (66%).

UV/Vis (DMSO): *λmax*: 421, 515, 555, 596, 645BHRMS (MALDI-TOF) calcd. for $C_{48}H_{30}N_4O_8$ $[M+ H]^+$ 791.21, found 791.35

Synthesis of Zinc-5,10,15,20-tetrakis-(4–carboxyl–methyl-phenyl) porphyrin (3)

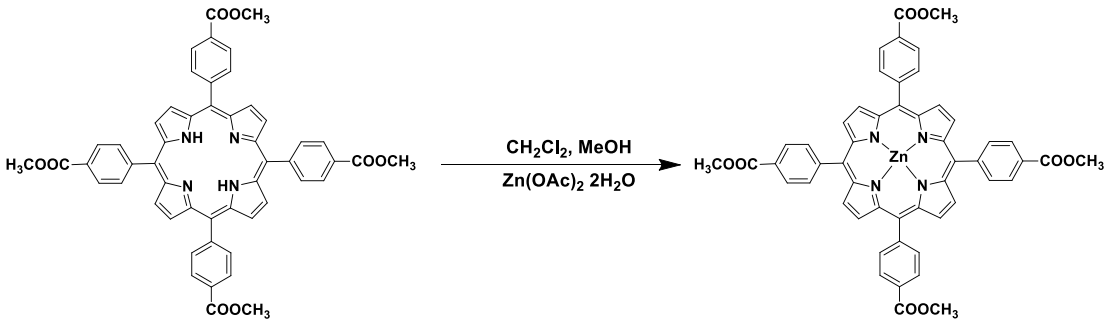

(1) (3)

In a solution of porphyrin (1) (220 mg, 0.26 mmol) in CH_2Cl_2 (67 mL) in a round bottom flask, a solution of $Zn(CH3COO)_2{\cdot}2H_2O$ (402.58 mg, 1.83 mmol) in MeOH (10 mL) was added and the reaction mixture was stirred at room temperature overnight. The crude product was purified by silica column chromatography eluting with CH_2Cl_2 – EtOH (98:2, v/v). Yield: 177 mg (75%).

UV/Vis (CH_2Cl_2): *λmax*: 421, 549, 587 HRMS (MALDI-TOF): m/z calcd. for $C_{52}H_{36}N_4O_8Zn$ [M] 908.18, found 908.33.

Synthesis of Zinc-5,10,15,20-tetrakis-(4–carboxy-phenyl) porphyrin (4)

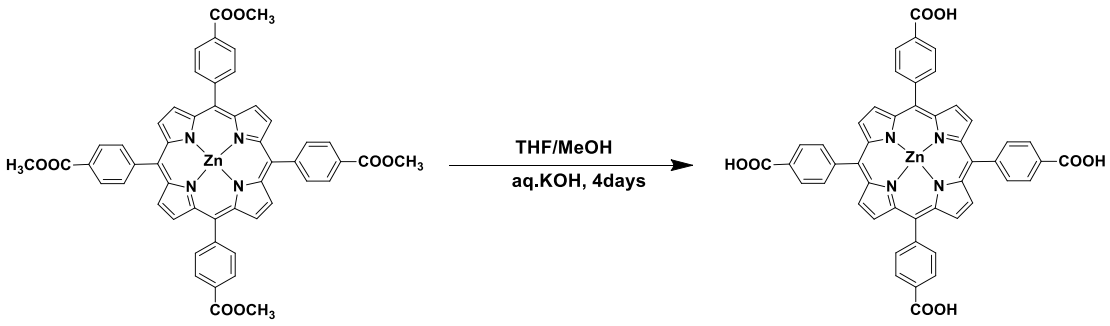

(3) (4)

In a round bottom flask, porphyrin (3) (65 mg, 0.24 mmol) was dissolved in THF (17 mL) and MeOH (7.5 mL). To this solution, KOH (500 mgr, 14.2 mmol) and distilled water (9 mL) were added and the reaction mixture was stirred at room temperature for 4 days. The solvents, THF and MeOH were completely removed on a rotary evaporator. The rest of the mixture was acidified with HCl 1 M (pH 5). The precipitate was filtered and washed with distilled water many times. Yield: 56 mg (86%).

UV/Vis (DMSO): *λmax*: 430, 561, 601 HRMS (MALDI-TOF): m/z calcd. for $C_{48}H_{28}N_4O_8Zn$ [M] 852.12, found 852.31.

Synthesis of diethyl–4–aldehydephenylphosphonate (5)

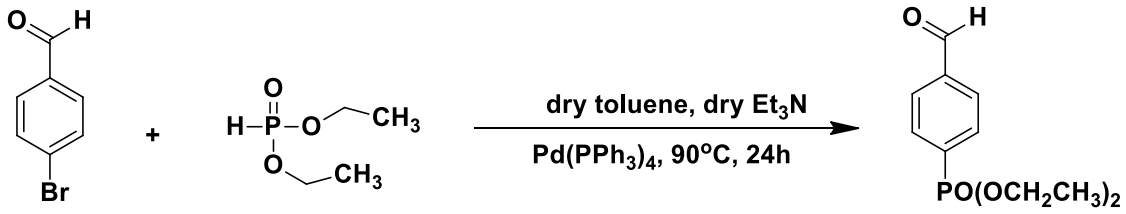

(5)

4-bromobenzaldehyde (500 mg, 2.70 mmol) was taken in a 100 mL two-necked bottom flask. To this solution, dry toluene (4 mL), dry Et_3N (4 mL) and diethylphosphite (0.4 mL, 6 mmol) were added and purged with Ar gas for 2 min. Finally, $Pd(PPh_3)_4$ (155 mg, 0.135 mmol) was added and the reaction mixture heated to 90 ^oC for 24 h under Ar atmosphere. The reaction mixture was cooled to room temperature and the solvent evaporated to

dryness under vacuum, re-dissolved in CH_3Cl (35 mL), washed with distilled water (3 × 50 mL), followed by brine solution (50 mL), and finally dried over with Na_2SO_4. The crude product was purified on a silica column chromatography using CH_3Cl – EtOAc (70:30, v/v) as the eluent. Yield: 300 mg (47%).

^{1}H NMR (300 MHz, $CDCl_3$): δ 10.09 (s, 1H, CHO), 8.00(m, 4H, ph-H), 4.15(m, 4H, -CH_2), 1.33(t, J=6.9Hz, 3H), 1.35(t, J=7.2Hz, 3H).

Synthesis of 5,10,15,20-tetrakis-(4-di-ethyl-phosphonate-phenyl) porphyrin (6)

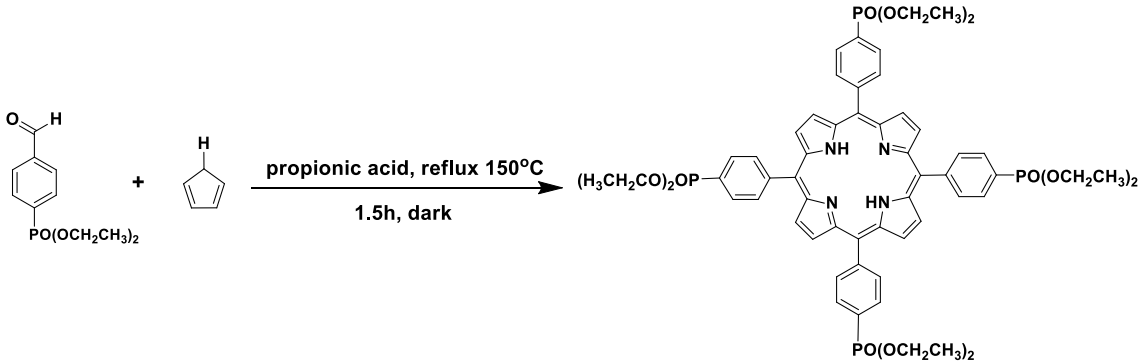

(6)

A solution of aldehyde (5) (280 mg, 1.18 mmol) and pyrrole (0.080 mL, 1.15 mol) in 10mL of propionic acid was refluxed at 150 ^{o}C in a flask protected from light for 1.5 h. The mixture was evaporated to dryness, and purified by column chromatography on neutral alumina eluting with CH_2Cl_2 – MeOH (99:1, v/v). Yield: 92.4 mg (6.7%).

UV/Vis (CH_2Cl_2): *λmax*: 419, 514, 549, 589, 645 HRMS (MALDI-TOF): m/z calcd. for $C_{60}H_{66}N_4O_{12}P_4$ $[M + H]^+$ 1159.36, found 1159.72

^{1}H NMR (300 MHz, $CDCl_3$): δ 8.84 (s, 8H, pyr), 8.34 (q, 8H, *o*-ph), 8.23(q, 8H, *m*-ph), 4.34(m, 16H, -OCH_2), 1.53(m, 24H, -CH_3)

Synthesis of 5,10,15,20-tetrakis-(4-phosphonato-phenyl) porphyrin (7)

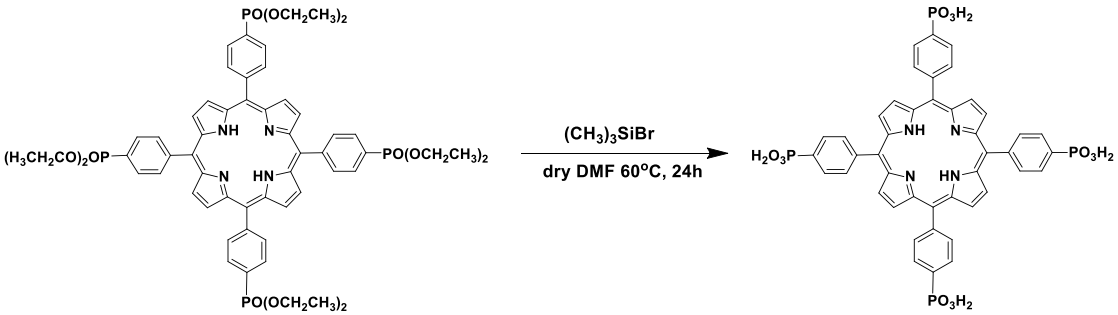

(6) (7)

In a two-necked bottom flask, a solution of porphyrin (6) (20 mg, 0.0172 mmol) and CH_3SiBr (0.1 mL, 0.76 mmol) in dry DMSO (4 mL) was heated under Ar atmosphere at 60 ^{o}C for 24 h. The solvent was evaporated under vacuum and the green solid residue was dissolved in MeOH and stirred at room temperature for 1 h. Et_2O was added until precipitation occurred, and the resulting solid was filtered off, washed with Et_2O and dried under vacuum. Yield: 16 mg (99%)

UV/Vis (H_2O): *λmax*: 414, 515, 549, 589,645 HRMS (MALDI-TOF): m/z calcd. for $C_{44}H_{34}N_4O_{12}P_4$ $[M + H]^+$ 935.11, found 935.24.

Synthesis of Zinc-5,10,15,20-tetrakis-(4-di-ethyl-phosphonate-phenyl) porphyrin (8)

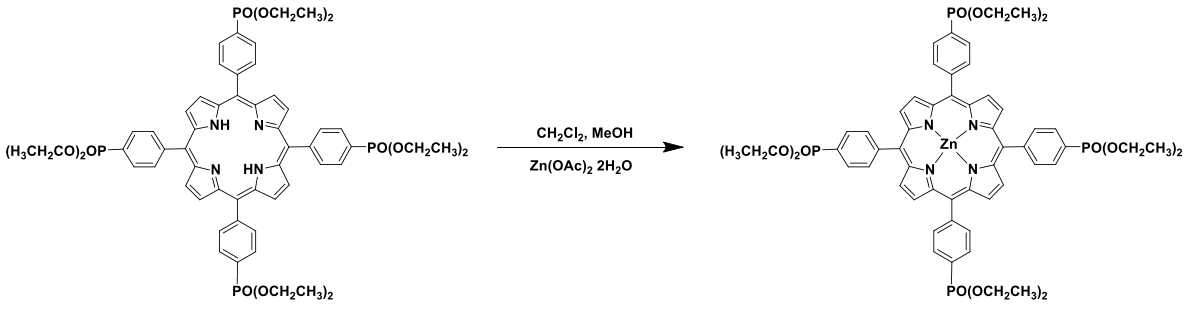

(6) (8)

In a solution of porphyrin (6) (20 mg, 0.0172 mmol) in CH_2Cl_2 (20 mL) in a round bottom flask, a solution of Zn(CH3COO)2·2H2O (38 mg, 0,173 mmol) in MeOH (3 mL) was added and the reaction mixture was stirred at room temperature overnight. The crude

product was purified by silica column chromatography eluting with CH_2Cl_2 – MeOH (98:2, v/v). Yield: 177 mg (75%).)

UV/Vis (CH_2Cl_2): *λmax*: 420, 548, 587 HRMS (MALDI-TOF): m/z calcd. for $C_{60}H_{66}N_4O_{12}P_4$ [M] 1220.28, found 1220.74

Synthesis of Zinc-5,10,15,20–tetrakis-(4-phosphonato-phenyl) porphyrin (9)

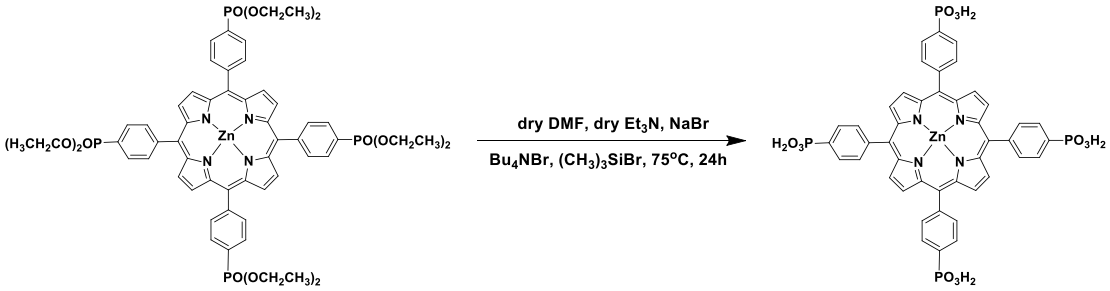

(8) (9)

In a round-bottom flask, porphyrin (6) (20 mg, 0.0164 mmol), Bu_4NBr (2.1 mg, 0.0066 mmol), dry Et_3N (114 µL), $(CH_3)_3SiBr$ (86.5 µL), NaBr (50.6 mg, 0.49 mmol) in dry DMF (2 mL) was heated under Ar atmosphere at 75 ^oC for 24h. The mixture was filtered off on celite with CH_2Cl_2, the solvents were evaporated under vacuum and the green solid residue was dissolved in MeOH and stirred at room temperature for 1 h. Et_2O was added until precipitation occurred, and the resulting solid was filtered off, washed with Et_2O and dried under vacuum. Yield: 14 mg (70%).

UV/Vis (H_2O): *λmax*: 421, 556, 596 HRMS (MALDI-TOF): m/z calcd. for $C_{44}H_{32}N_4O_{12}P_4Zn$ $[M+H]^+$ 996.03, found 997.17.

Synthesis of Tetrakis-[4-(4-ethoxy-4-oxobutoxy)phenyl] porphyrin (10)

The Tetrakis-[4-(4-ethoxy-4-oxobutoxy)phenyl] porphyrin was synthesized following the literature procedure [41].

Synthesis of Zinc-tetrakis-[4-(4-ethoxy-4-oxobutoxy)phenyl] porphyrin (11)

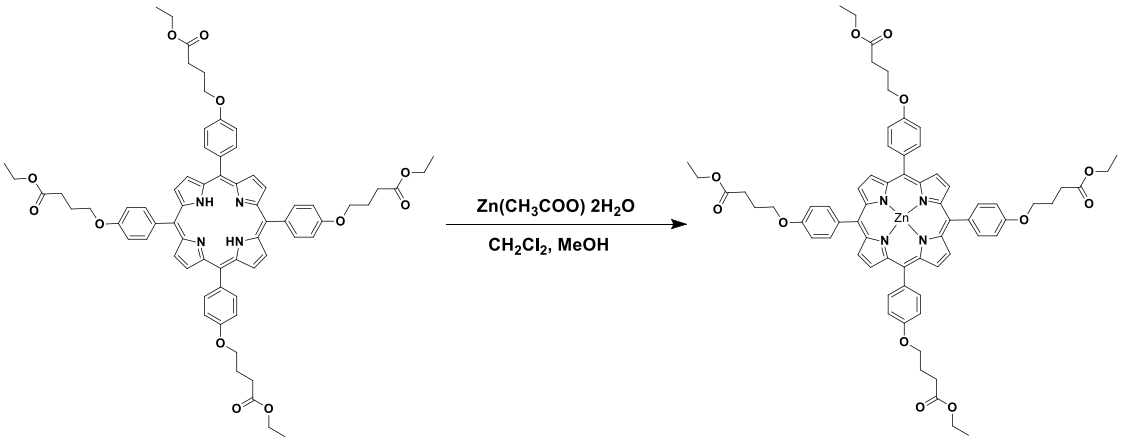

In a solution of porphyrin (10) (25 mg, 0.022 mmol) in CH_2Cl_2 (25 mL) in a round bottom flask, a solution of $Zn(CH_3COO)_2{\cdot}2H_2O$ (48 mg, 0,22 mmol) in MeOH (3.5 mL) was added and the reaction mixture was stirred at room temperature overnight. The crude product was purified by silica column chromatography eluting with CH_2Cl_2 – MeOH (99:1, v/v). Yield: 20 mg (77%).

UV/Vis (CH_2Cl_2): *λmax*: 422, 518, 556, 594, 651 HRMS (MALDI-TOF): m/z calcd. for $C_{64}H_{60}N_4O_{12}Zn$ $[M + H]^+$ 1197.41, found 1197.10

^1H NMR (300 MHz, $CDCl_3$): δ 8.97 (s, 8H, pyr), 8.11 (d, J=8.4Hz, 8H, *o*-Ar), 7.25(d, J=7.5Hz, 8H, *m*-ph), 4.34(m, 16H, $-OCH_2$), 1.53(m, 24H, $-CH_3$)

Synthesis tetrakis-[4-(4-oxobutoxyl)phenyl] porphyrin (12)

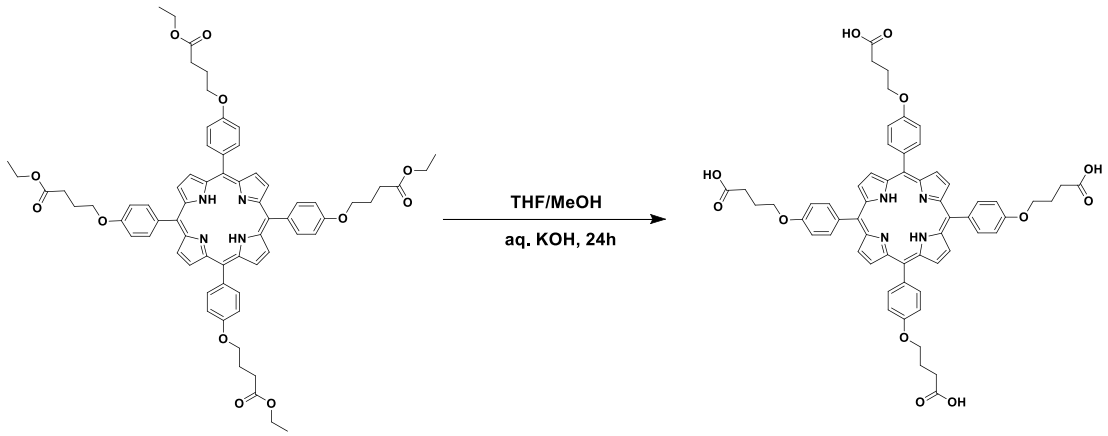

(10) (12)

In a round bottom flask, porphyrin (10) (50 mg, 0.044 mmol) was dissolved in THF (86 mL) and MeOH (35 mL). To this mixture, a solution of aq. KOH 0.5 M (36 mL) were added and the reaction mixture was stirred at room temperature for 24 h. The solvents, THF and MeOH were completely removed on a rotary evaporator. The rest of the mixture was acidified with HCl 1 M (pH 3). The precipitate was filtered and washed with distilled water many times. Yield: 36 mg (80%). UV/Vis (DMSO): *λmax*: 423, 519, 557, 595, 652 HRMS (MALDI-TOF): m/z calcd. for $C_{60}H_{54}N_4O_{12}$ $[M+H]^+$ 1022.37, found 1023.67

Synthesis Zinc-tetrakis-[4-(4-oxobutoxyl)phenyl] porphyrin (13)

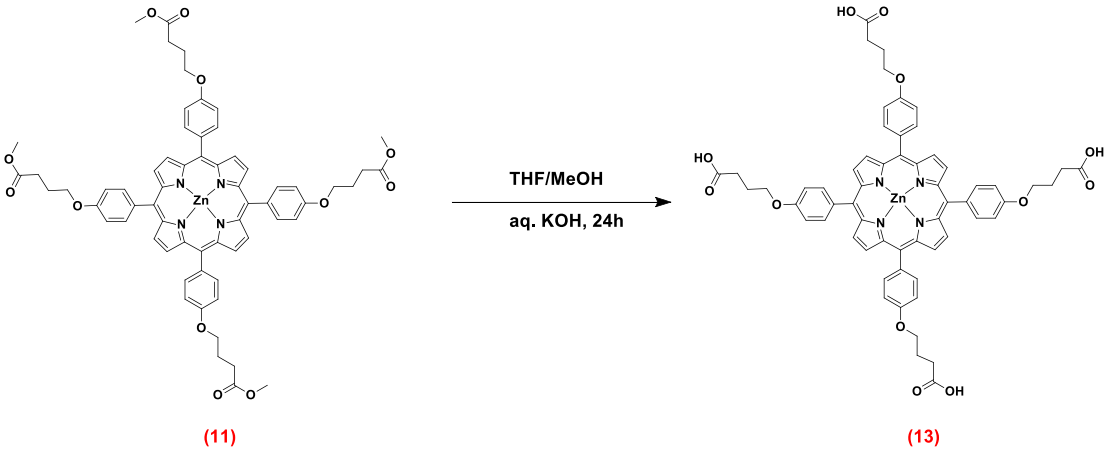

(11) (13)

In a round bottom flask, porphyrin (11) (15 mg, 0.013 mmol) was dissolved in THF (26 mL) and MeOH (11 mL). To this mixture, a solution of aq. KOH 0.5 M (11 mL) were added and the reaction mixture was stirred at room temperature for 24 h. The solvents, THF and MeOH were completely removed on a rotary evaporator. The rest of the mixture was acidified with HCl 1 M (pH 3). The precipitate was filtered and washed with distilled water many times. Yield: 11.3 mg (80%).

UV/Vis (DMSO): *λmax*: 431, 562, 604 HRMS (MALDI-TOF): m/z calcd. for $C_{60}H_{52}N_4O_{12}Zn$ [M] 1084.29, found 1084.76

Synthesis of 5,10,15–(4–carboxyl-phenyl) corrole (14)

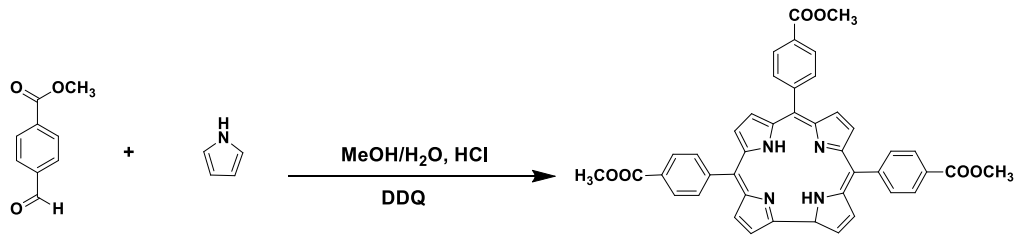

(14)

In a mixture of 200 mL of MeOH – distilled water (50:50 v/v), methyl 4-formylbenzoate (820 mg, 5 mmol), pyrrole (0.67 mL, 10 mmol) and HCl (5 mL, 0.25 mmol) were mixed together. The reaction mixture was stirred at room temperature under air for 3 h. Then, the mixture was extracted with CH_2Cl_2 (2×100 mL), the organic phase was collected and washed with distilled water (2×100 mL), dried over with Na_2SO_4 and then oxidized with DDQ (1 gr, 4.4 mmol) under stirring for 1h at room temperature. The crude product was purified by chromatography silica gel using CH_2Cl_2 - MeOH (99:1, v/v). Yield: 2.22 gr (68%).

UV/Vis (CH_2Cl_2): *λmax*: 423, 580, 620 HRMS (MALDI-TOF): m/z calcd. for $C_{43}H_{32}N_4O_6$ $[M+H]^+$ 701.23, found 701.64

Synthesis of 5,10,15–(4–carboxy-phenyl) corrole (15)

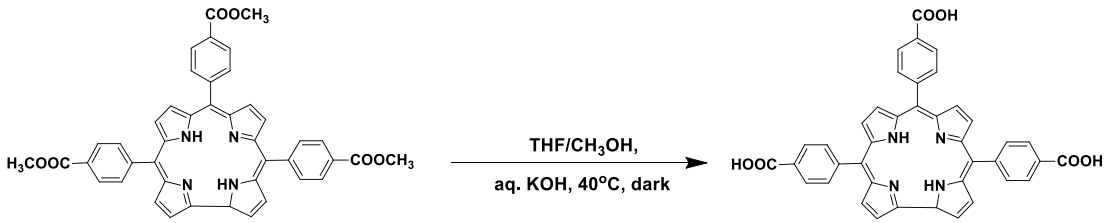

(14) (15)

Corrole (17) (15 mg, 0.023 mmol) was dissolved in a mixture of THF/CH_3OH (30 mL, 1:2) and 40% aq. KOH (1.9 mL). The solution was protected from light and stirred at 40 ^oC under N_2. The reaction progress was monitored on TLC. After all ester was consumed (only start spot on TLC), the reaction mixture was cooled down and acidized with HCl. The product was extracted with THF - CH_2Cl_2 (40 mL, 1:1), the organic phase was collected and washed with water (3×50 mL), dried over with Na_2SO_4, filtered and evaporated. The crude product was purified by crystallizing from acetone/hexane (1:2.5). Yield: 7.2 mg (48%).

UV/Vis (CH_2Cl_2): *λmax* 411, 562, 611 HRMS (MALDI-TOF): m/z calcd. for $C_{40}H_{26}N_4O_6$ $[M + H]^+$ 659.19, found 659.23

Synthesis of 5,15-(bis-pentafluoro-phenyl)-10-(carboxyl-methyl)phenyl corrole (16)

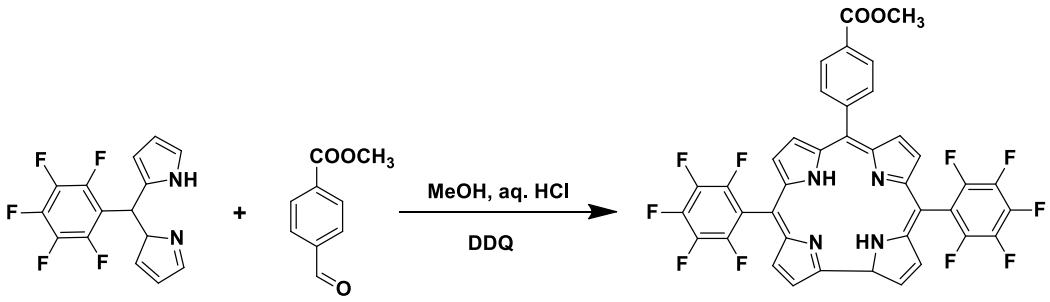

(16)

In a round bottom flask, dipyrromethane (753 mgr 2.5 mmol) and aldehyde (205 mgr, 1.25 mmol) were dissolved in MeOH and 130 mL of 20% aq. HCl was added. The mixture was left stirring for 1h at room temperature. The product was extracted with CH3Cl (2×50 mL) and the organic phase was collected and washed with water (2×50 mL), dried over with Na_2SO_4, filtered and condensed in the final volume of 20 mL. Then, 20 mL of

solution of DDQ (750 mg, 3.30 mmol) in toluene-CH_2Cl_2 (75:25, v/v) were added and the mixture was stirred for 30 min at room temperature. The crude product was purified by silica column chromatography eluting with CH_2Cl_2 -hexane (50:50, v/v). Yield: 260 mg (28%)

UV/Vis (CH_2Cl_2): *λmax:* 411, 563, 611 HRMS (MALDI-TOF): m/z calcd. for $C_{39}H_{18}F_{10}N_4O_2$ [M] 764.13, found 764.33

Synthesis of 5,15-(bis-pentafluoro-phenyl)-10-(carboxy-phenyl) corrole (17)

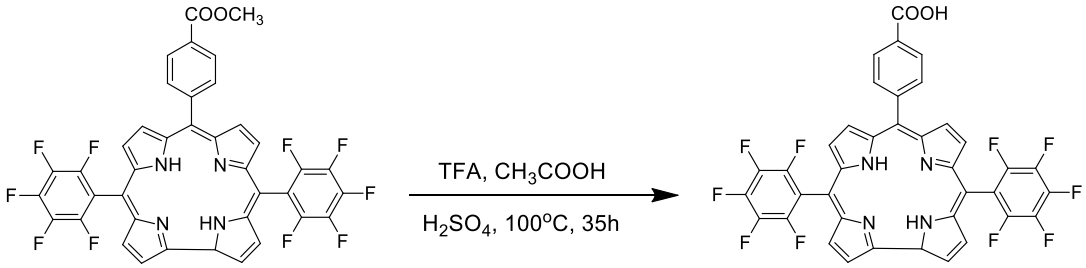

(16) **(17)**

In a two-necked bottom flask, a solution of corrole (19) (10 mg, 0.0133 mmol), TFA (0.4 mL, 5.22 mmol), CH_3COOH (0.2 mL, 3.49 mmol) and 5% aq. H_2SO_4 (0.1 mL, 1.88 mmol) was heated under Ar atmosphere at 100 ^oC for 35 h in the dark. The reaction mixture cooled down and neutralized with $NaHCO_3$. The product extracted with CH_3Cl (1×50 mL), dried over Na_2SO_4, filtered and evaporated. Yield: 7 mg (70%).

UV/Vis (CH_2Cl_2): *λmax:* HRMS (MALDI-TOF): m/z calcd. for $C_{38}H_{16}F_{10}N_4O_2$ [M] 750.11, found 750.33

Synthesis of $Ru[(bpy)_2(H_4dpbpy)](ClO_4^-)_2$ complex (18)

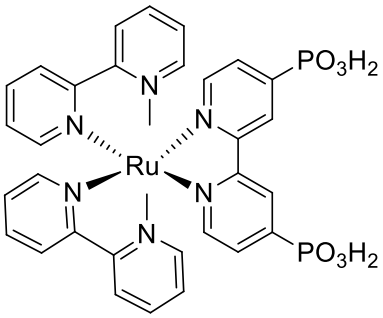

(RuP)

The $Ru[(bpy)_2(H_4dpbpy)](ClO_4^-)_2$ complex was synthesized following the literature procedure. [5]

Dioxygen Consumption Experiments

Materials. Purified water (Millipore: 18 MΩ cm) was buffered with triethanolamine (TEOA, 25 mM), which acted as sacrificial electron donor, and titrated with dilute HCl to the desired pH at the experimental temperature. The nanoparticles (AEROXIDE TiO_2 P25 particles from Evonik Industries) were an anatase/rutile (8:2) mixture with an average size of 21 nm.

Laccase Production. The laccase (LAC3 from fungus *Trametes* sp. strain C30)[27] is produced by heterologous expression of the laccase in the filamentous fungus *Aspergillus niger* in large – scale production (300 mg/L) as described elsewhere. Samples were kept in freezer in aqueous phosphate buffer pH 6.0 + 10% glycerol.

Dioxygen Consumption. Dioxygen consumption was measured by polarography using a YSL MODEL 5300 BIOLOGICAL OXYGEN MONITOR (Scientific Division Yellow Spings Instruments Co., Inc) with a micro Clark electrode fitted to a temperature controlled glass chamber. The sample was irradiated using Wolfram lamp (250 W) with a filter cuts off 400 nm (see **Scheme 3**).

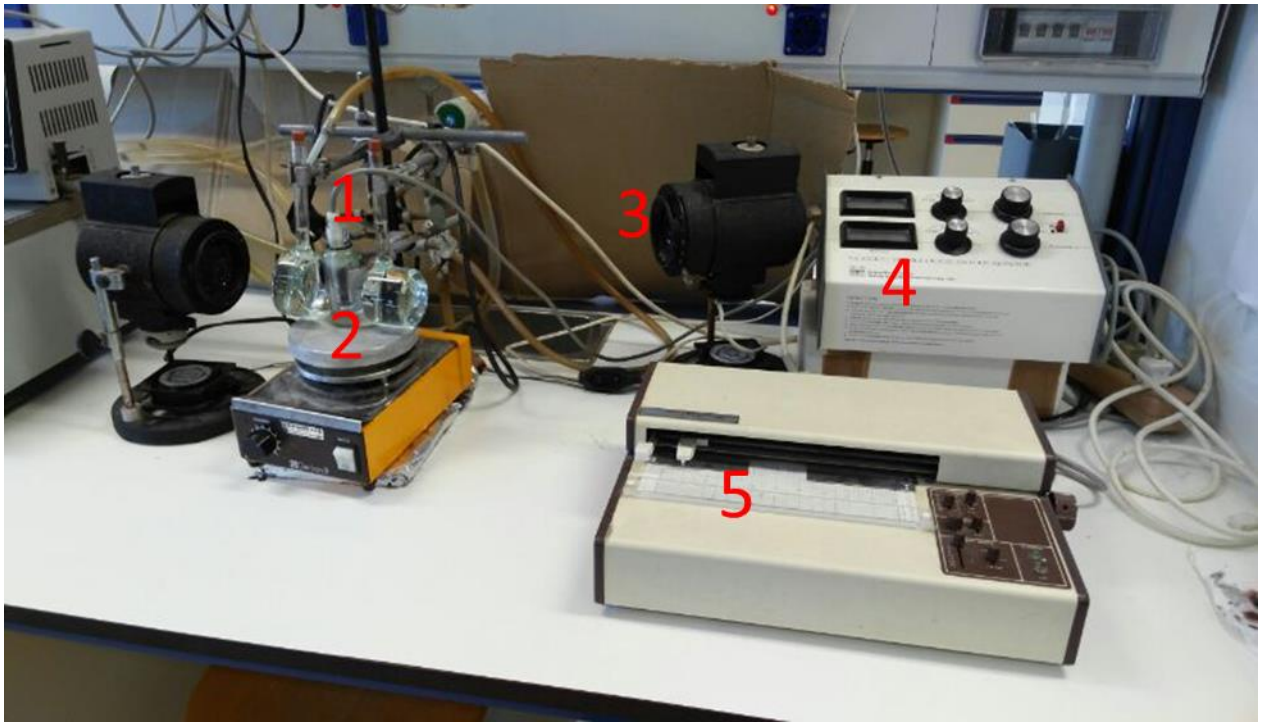

Scheme 3: Illustration of Clark electrode set up 1) Clark electrode, 2) glass chamber, 3) light source, 4) oximeter, 5) recorder.

Determination of Maximum Concentration of Enzyme Absorbed on TiO_2 nanoparticles

Our first goal was to find out which is the maximum concentration of laccase that can be attached to the TiO_2 nanoparticles. For this study, we prepared three samples with different concentration of enzyme 5 µM, 6 µM and 9 µM. Particularly, 9 mg of TiO_2 was sonicated in 1.5 mL of TEOA buffer, and laccase was then added to the stirred dispersion. The mixture was left stirring for 15 min, centrifuged and the filtered clear supernatant was then analyzed by UV-Vis spectrophotometry. The amount of absorbed laccase was quantified by the absorbance at 280 nm. We found out that in case of 5 µM, the whole enzyme has been bound on TiO_2 (no peak at 280 nm) compared to the other two cases where there is a peak at 280 nm, which means that there is free laccase. Finally, the maximum concentration of laccase attached to TiO_2 is 5 µM.

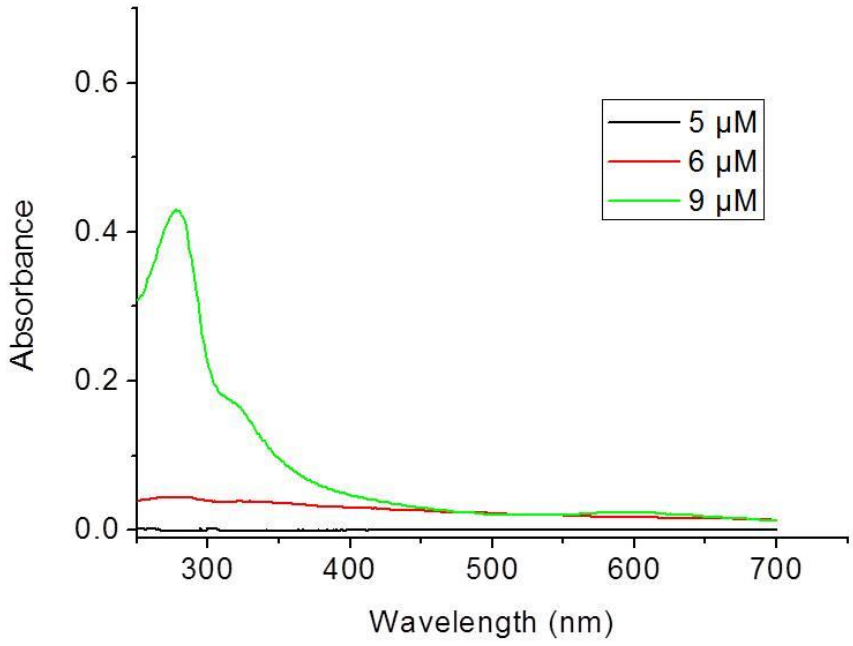

Figure 11: Absorption spectrum of different concentration of laccase on TiO_2 nanoparticles

We have to mention that when we left the sample with 9µM of enzyme stirring for 24h, the peak at 280nm increased.

Determination of the Time of Washing after the Attachment of Photosensitizer

In this part, we wanted to test if the time of stirring while washing, plays important role in our preparation of samples. Namely, we wanted to see if the amount of porphyrin attached to TiO_2 nanoparticles depends on time of stirring while washing. We tried three different approaches: 1) by hand (control A), 2) stirring bar for 5 min (control B) and 3) stirring bar for 15 min (control C).

Thus, 9 mg of TiO_2 was sonicated in 1.5mL of 25mM TEOA buffer for 3min, and amount of dye solution (0.1 µmol) was then added to the stirred dispersion. The mixture was left stirring, centrifuged, and the filtered clear supernatant was then analyzed by UV-Vis spectrophotometry. The amount of absorbed dye was quantified by the absorbance at Soret

band. Observing the spectrums, we found out that they are identical. In other words, the time of stirring while washing does not affect the absorption of porphyrin on TiO_2.

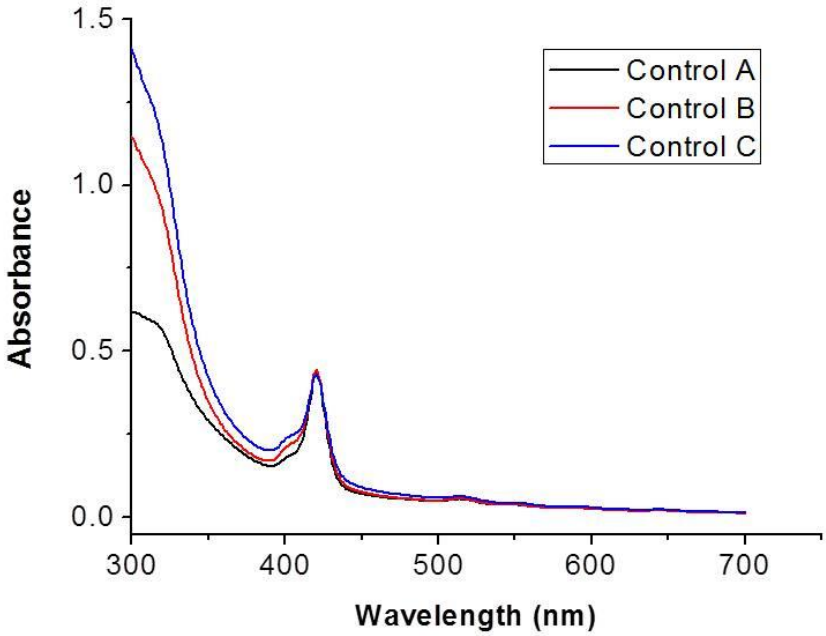

Figure 12: Absorption spectrum of control experiments for different time of washing after the attachment of photosensitizer

Preparation of Samples

First, 9 mg of TiO_2 nanoparticles are sonicated in 1.5 mL of 25 mM TEOA buffer pH 6 for 3 min followed by addition of laccase and stirring for 15 min under protection from light. The particles are separated from the supernatant solution by centrifugation. All the amount of nanoparticles is then sonicated with fresh 1.5 mL of 25 mM TEOA buffer pH 6 for 5min and the photosensitizer solution is added. The mixture is left stirring for 15 min and then the particles are separated from the supernatant solution by centrifugation. Nanoparticles are sonicated again in 1.5 mL of 25 mM TEOA buffer pH 6 for 5 min and left stirring for 5 min. The particles are separated from the supernatant solution by centrifugation. All the

amount of particles is resuspended in 1.5 mL of fresh 25 mM TEOA buffer pH 6. The sample is kept in the freezer until the measurement.

It is important to mention that some of the photosensitizers are not soluble in water which means that we need to find other solvent to make their stock solutions. Porphyrin (9) and RuP complex are water soluble so their stock solutions are in TEOA buffer. Contrariwise, porphyrins (2), (4), (12), (13) and the two corroles (9), (11) the stock solutions are in DMSO. That means that during the preparation of the samples, after the attachment of the photosensitizer, nanoparticles are sonicated again in 1.5 mL of DMSO for 5 min and left stirring for 5 min. The particles are separated from the supernatant solution by centrifugation. All the amount of nanoparticles are sonicated again in 1.5 mL of 25 mM TEOA buffer pH 6 for 5 min and left stirring for 5 min. The particles are separated from the supernatant solution by centrifugation. All the amount of particles resuspended in 1.5 mL of fresh 25 mM TEOA buffer pH 6. The sample is kept in the freezer until the measurement.

Absorption of Laccase on TiO_2 nanoparticles

The attachment of laccase to the TiO_2 nanoparticles, is verified by monitoring the absorbance at 280 nm of supernatant solution comparing to a laccace control solution.

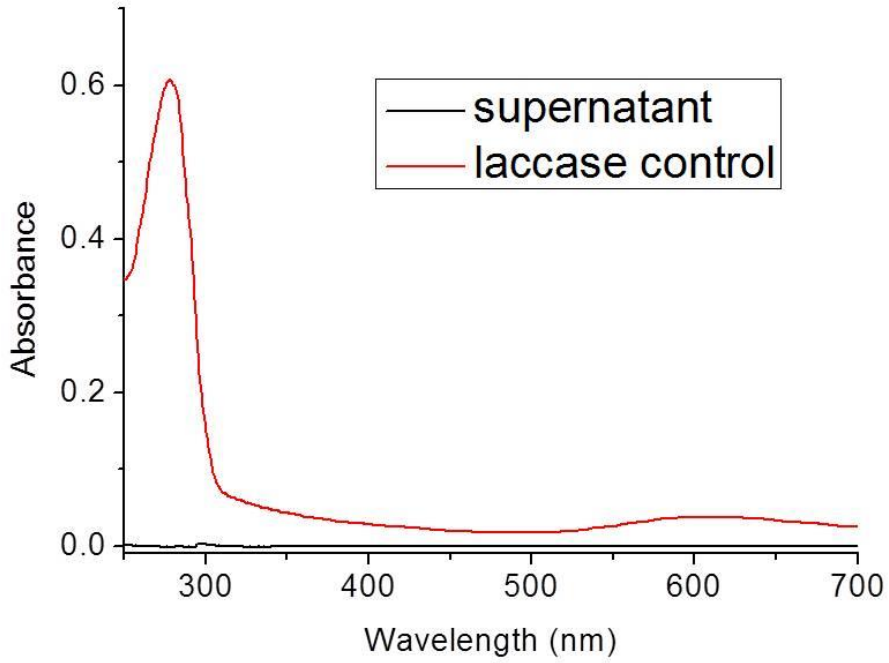

Figure 13: Absorption spectra of laccase before and after its attachement on TiO_2 nanoparticles

Absorption of Photosensitizer on TiO_2 nanoparticles

The attachment of photosensitizer to the TiO_2 nanoparticles, is verified by monitoring the absorbance of supernatant solution comparing to a photosensitizer (PS) control solution.

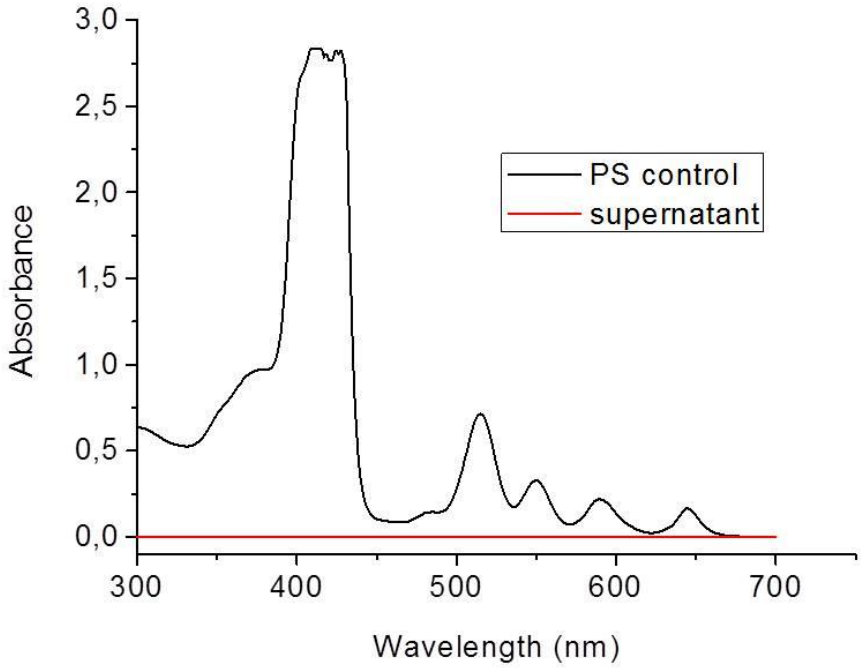

Figure 14: Absorption spectra of photosensitizer before and after its attachment on TiO_2 nanoparticles

Furthermore, the amount of absorbed dye was quantified by the absorbance difference at Soret or Q band of the supernantant after washing with DMSO or TEOA buffer and the photosensitizer (PS) control solution.

Procedure of Dioxygen Consumption Measurement

The standard procedure of dioxygen consumption measurement consists of the following steps: firstly, 1450 µL of 25 mM TEOA buffer pH 6 and 50 µL of the sample were added into the glass chamber of the electrode. Then, we adjust the electrode and leave the system for a while to stabilize without irradiation. The whole system is protected from the light. After that, the system was irradiated for 2 min using a filter cutting wavelengths below 420 nm. For each sample, the experiment was carried out three times. In the absence of light no dioxygen consumption was detected under the same experimental conditions.

Control experiments established the following: sample containing only TiO_2 without absorbed enzyme or photosensitizer did not show dioxygen consumption, sample containing only TiO_2 with absorbed enzyme showed a small rate of dioxygen consumption around ~ 6 μmol/L/min.

Photocatalysis Experiments

Photocatalysis experiments

In this part, oxidation reactions were carried out in order to achieve visible - driven oxidation of an alkene to epoxide mediated by photosensitizer/TiO_2/laccase system with O_2 as oxidant. The reaction takes place in water at room temperature and, importantly, without any sacrificial electron acceptor (**Scheme 1**). The epoxyde derived from the oxygenation of the p-styrene sulfonate (substrate) as well as the secondary products, the diol resulting from a spontaneous opening of the epoxide ring and the p-benzaldehyde sulfonate probably resulting from an oxidation of the diol were independently assayed as substrate in dioxygen consumption experiments.

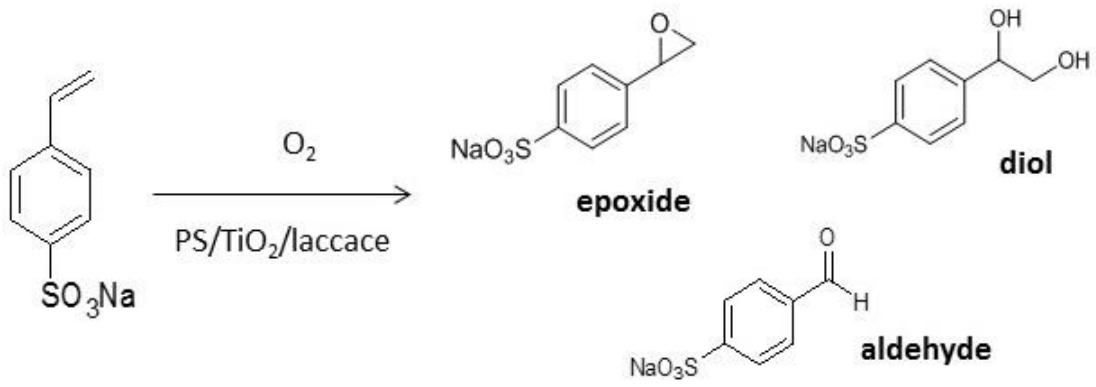

Scheme 4: Photooxidation reaction of p-styrene sulfonate and its products.

Experimental Procedure

50 µL of sample photosensitizer/TiO_2/laccase was added in a buffered solution (Britton Robinson buffer (B&R) pH 6) at 25°C containing 25 mM of p-styrene sulfonate. The mixture was left stirring under white light irradiation using filter (λ > 450 nm) for 24 h. The formation of oxidized species was analyzed by ^{1}H NMR.

Chapter 3

Results and Discussion

Dioxygen Consumption Measurements

The principle of the system depicted in **Scheme 1** is that visible light excites the photosensitizer, which injects one electron at a time into the TiO_2 conduction band (the oxidized dye is recovered by the sacrificial electron donor); electrons are then transferred into the active site of enzyme at which four electrons as well as four protons are used to reduce a molecule of dioxygen with the concomitant formation of two water molecules.

In this part, the results of visible light – driven dioxygen consumption measurements are presented for each system that we study. Before we proceed to the results I would like to mention that the concentrations of laccase and photosensitizers in the following tables correspond to the concentration of each of them inside the glass chamber of the Clark electrode that we used for our dioxygen consumption measurements.

Dioxygen consumption measurements using porphyrin (2) as photosensitizer

As it is mentioned in the part of ***Determination of Maximum Concentration of Enzyme Absorbed on TiO_2 nanoparticles,*** the maximum concentration of laccase that can be absorbed on TiO_2 nanoparticles is 5 μM. Six samples of photosensitizer/TiO_2/laccase were prepared containing 5 μM of laccase and various concentrations of photosensitizer. The results are shown in **Table 2**.

Laccase	Photosensitizer	Consumption (μmol O_2 / L / min)
167 nM	4.4 μM	20
167 nM	2.2 μM	20
167 nM	1.1 μM	18
167 nM	0.44 μM	11
167 nM	0.22 μM	8
167 nM	0.088 μM	5

Table 2: The effect of various ratios of porphyrin (2) in system photosensitizer/TiO_2/laccase on dioxygen consumption during 2min irradiation in TEOA buffer (25 mM, 1.5 mL) at pH 6 and 25 ^{o}C.

For the above samples, with the exception of the first one, the amount of photosensitizer attached to TiO_2 nanoparticles after washing is around 65% of the initial

amount. Sensitizing the TiO_2 particles with higher concentration of porphyrin (2), resulted in the absorption of only 60% of the initial porphyrin. For this reason, we did not performed experiments with excess of photosensitizer.

So, we first investigated various concentrations of photosensitizer. Increasing the amount of porphyrin (2), the dioxygen consumption is increasing too. This indicates that since more molecules of photosensitizer are excited, more electrons are injected into the TiO_2 conduction band and so more molecules of the enzyme are capable to accept the electrons and reduce the dioxygen molecules. However, over 1.1 μM of photosensitizer, the rate of consumption remains almost stable. A plausible explanation for this behavior is that subsequent addition of photosensitizer does not produce further consumption. On the contrary, for those ratios the system is saturated which means that there are no extra, available molecules of the enzyme to receive electrons and reduce dioxygen.

At the same time, the dioxygen consumption of sample containing photosensitizer/TiO_2 was also measured and found 15 μmol/ L/ min.

Taking into consideration the amount of the attached photosensitizer and the results of dioxygen consumption, the operational conditions for the system *porphyrin (2)/TiO_2/laccace* leading to optimal performance (18 μmol/L/min), are found to be 167 nM of laccase and 2.2 μM of photosensitizer. In presence of 100eq NaF, inhibitor, the comsuption decreases and the rate reaches 13 μmol/ L/ min. Moreover, control experiments indicate that the combination of laccase with photosensitizer enhance the dioxygen consumption, as the photosensitizer shows high effectiveness compared to laccase itself.

Next, we evaluated the effectiveness of various concentrations of laccase in dioxygen consumption. Six samples of photosensitizer/TiO_2/laccase were prepared containing 2.2 μM of photosensitizer and various ratios of enzyme. The results are shown in **Table 3**.

Laccase	Photosensitizer	Consumption (μmol O_2 / L / min)
167 nM	2.2 μM	20
83.5 nM	2.2 μM	17
16.7 nM	2.2 μM	14
8.35 nM	2.2 μM	12
3.34 nM	2.2 μM	10
1.67 nM	2.2 μM	10

Table 3: The effect of various ratios of laccase in system photosensitizer/TiO_2/laccase on dioxygen consumption during 2min irradiation in TEOA buffer (25 mM, 1.5 mL) at pH 6 and 25 ^{o}C.

It is clear that by decreasing the amount of laccase, the dioxygen consumption rate is decreasing too. This is likely due to the less attached molecules of enzyme to TiO_2 surface. So, less molecules of dioxygen are reduced. Although the sample containing 167 nM of laccase did not exhibit the same rate of dioxygen consumption as shown in Table 1, it is still high.

In order to investigate the reproducibility and effectiveness of the system, fresh samples were prepared. Moreover, instead of using 50 μL of sample, this time 100 μL of sample were added into the glass chamber for a final volume 1.5 mL of 25 mM TEOA buffer pH 6. The results are represented in **Table 4**.

Laccase	Photosensitizer	Consumption (μmol O_2 / L / min)
167 nM	2.2 μM	19
-	2.2 μM	14
334 nM	4.4 μM	37
-	4.4 μM	27

Table 4: Dioxygen consumption results in system photosensitizer/TiO2/laccase during 2min irradiation in TEOA buffer (25 mM, 1.5 mL) at pH 6 and 25 ^{o}C.

The dioxygen consumption rate was enhanced almost two-fold when the amount of sample was increased from 50 μL to 100 μL. Moreover, the obtained results verify that we have reproducibility in our measurements.

We also studied the bimolecular system. In other words the system was prepared by mixing photosensitizer and laccase in solution. The results of dioxygen consumption are shown in **Table 5.**

Laccase	Photosensitizer	Consumption (µmol O_2 / L / min)
167nM	2.2 µM	10
30 µM	30 µM	23
-	30 µM	15

Table 5: Dioxygen consumption results in bimolecular system photosensitizer/laccase during 2 min irradiation in TEOA buffer (25 mM, 1.5 mL) at pH 6 and 25 ^{o}C.

Comparing the system photosensitizer/TiO_2/laccase to bimolecular system with the same concentration (167 nM laccase, 2.2 µM photosensitizer), it is obvious that the dioxygen consumption rate in the case of former is higher. Therefore, electron transfer between porphyrin and laccase via TiO_2 is faster than that via the bimolecular system.

The dioxygen consumption rate in bimolecular system (30 µM:30 µM) is much higher comparing to the control sample containing only porphyrin in the same concentration. This indicates that the porphyrin plays an important role in the efficacy of our system.

Dioxygen consumption measurements using porphyrin (7) as photosensitizer

Apart from carboxylate groups, phosphonate groups are another candidate for strong binding in TiO_2 nanoparticles. For this reason, we wanted to investigate another photosensitizer bearing phosphonate groups. So we chose porphyrin (7). The same preparation process of sample was followed.

It is worth noting that the porphyrin (7) is water soluble. That means that during the preparation process of samples with this porphyrin, the sample is washed only once with 25 mM TEOA buffer pH 6. The most important thing is that the whole amount (> 98 %) is absorbed on TiO_2 nanoparticles.

At first, three samples containing only photosensitizer/TiO_2 were prepared and the obtained dioxygen consumption rates are reported in **Table 6**.

Photosensitizer	Consumption (μmol O_2 / L / min)
8.8 μM	15
4.4 μM	21
2.2 μM	20

Table 6: Dioxygen consumption results of control experiments in system photosensitizer/laccase using porphyrin (7) during 2 min irradiation in TEOA buffer (25 mM, 1.5 mL) at pH 6 and 25 ^{o}C.

Even though in all three cases, all the amount of porphyrin is attached to TiO_2 surface, it is observed that by increasing the concentration of photosensitizer the dioxygen consumption rate is reducing. This behavior is likely attributed to saturation resulted in the formation of aggregates which prevent the injection of electrons into the conduction band of TiO_2.

Then, samples containing 2.2 μM of photosensitizer and varying amounts of enzyme were prepared and their dioxygen consumption measurements were carried out. The results are presented in **Table 7**.

Laccase	Photosensitizer	Consumption (μmol O_2/L/min)
167 nM	2.2 μM	28
16.7 nM	2.2 μM	34
0.167 nM	2.2 μM	32
0.0167 nM	2.2 μM	30
0.00167 nM	2.2 μM	29

Table 7: Dioxygen consumption results in system photosensitizer/TiO_2/laccase using porphyrin (7) during 2 min irradiation in TEOA buffer (25 mM, 1.5 mL) at pH 6 and 25 ^{o}C.

The above results obtained only once and every time that we tried to repeat the experiments we did not get reproducible rates. This could happen because of the loss of enzyme's activity. So, our next step was the preparation of new samples with fresh laccase.

The obtained results of dioxygen consumption measurements of new samples are summarized in **Table 8.**

Laccase	Photosensitizer	Consumption (µmol O_2 / L / min)
167 nM	2.2 µM	34
1.67 nM	2.2 µM	27.5
167 nM	1.1 µM	19.9
167 nM	0.22 µM	10.5
-	2.2 µM	26
-	1.1 µM	16
-	0.22 µM	8

Table 8: Dioxygen consumption results (new samples) in system photosensitizer/TiO_2/laccase using porphyrin (7) during 2 min irradiation in TEOA buffer (25 mM, 1.5 mL) at pH 6 and 25 °C.

The optimal performance of the system was obtained with the concentration of 167 nM of laccase and 2.2 µM of photosensitizer. Decreasing the amount of enzyme hundred times, the dioxygen consumption rate is presenting a small decrease (27.5 µmol O_2 / L / min). This indicates that the rate of dioxygen consumption is not proportional to the concentration of the enzyme.

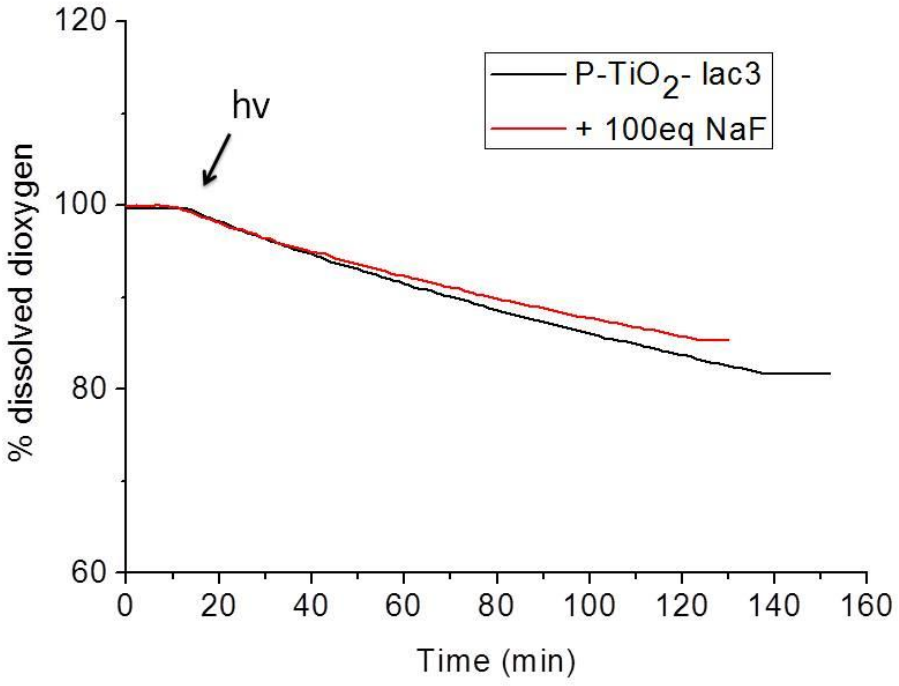

Figure 15: Dioxygen consumption rate in absence (–) and presence (–) of NaF in porphyrin (7)/TiO_2/laccase system

Moreover, it is obvious that the same rate of dioxygen consumption is also obtained in control experiment including only porphyrin in the same ratio. This means, that in the particular system photosensitizer/TiO_2/laccase, the effectiveness of the enzyme is almost absent. On the other hand, by reducing the amount of photosensitizer ten times, a dramatic reduction of dioxygen consumption rate is observed. Taking into consideration the fact that all the amount of porphyrin is bound to TiO_2 it seems that a decrease of photosensitizer causes a decrease in number of electrons injected to TiO_2 and then to the active site of laccase.

The experiments were conducted in the presence of sodium fluoride, a strong inhibitor of laccases. Upon irradiation of solutions containing amount of sample, TEOA buffer and 100 eq of NaF, the dioxygen consumption decreased and the rate reached 28 μmol/L/min.

Experiments of dioxygen consumption in the presence of the bimolecular system were also performed. The results are shown in **Table 9.**

Laccase	Photosensitizer	Consumption (μmol O_2 / L / min)
167 nM	2.2 μM	10
30 μM	30 μM	24
-	30 μM	15.7

Table 9: Dioxygen consumption results in bimolecular system photosensitizer/laccase during 2 min irradiation in TEOA buffer (25 mM, 1.5 mL) at pH 6 and 25 ^{o}C.

Comparing the system photosensitizer/TiO_2/laccase to bimolecular system with the same concentration (167 nM laccase, 2.2 μM photosensitizer), it is obvious that the dioxygen consumption rate in the case of former is higher. Therefore, electron transfer between porphyrin and laccase via TiO_2 is faster than that via the bimolecular system.

The dioxygen consumption rate in bimolecular system (30 μM: 30 μM) is much higher compared to the control sample containing only porphyrin in the same concentration. This indicates that the porphyrin plays an important role in the efficacy of our system.

The dioxygen consumption rates in bimolecular system using porphyrin (7) are similar to the ones of bimolecular system using porphyrin (2).

Dioxygen consumption measurements using RuP complex as photosensitizer

For comparison reasons, dioxygen consumption experiments were performed using a RuP complex bearing two phosphonic groups. All the amount of photosensitizer is absorbed on TiO_2 surface (> 98 %) The results of dioxygen consumption for systems **photosensitizer/TiO_2/ laccase** and bimolecular system **photosensitizer/laccase** are shown in **Table 10** and **Table 11** respectively.

Laccase	Photosensitizer	Consumption (µmol O_2 / L / min)
167 nM	2.2 µM	33
-	2.2 µM	25

Table 10: Dioxygen consumption results in system photosensitizer/TiO_2/ laccase using RuP during 2 min irradiation in TEOA buffer (25 mM, 1. 5mL) at pH 6 and 25 °C.

Laccase	Photosensitizer	Consumption (µmol O_2 / L / min)
167 nM	2.2 µM	25
30 µM	30 µM	22
-	30 µM	16.5

Table 11: Dioxygen consumption results in bimolecular system photosensitizer/laccase using RuP complex during 2 min irradiation in TEOA buffer (25 mM, 1.5 mL) at pH 6 and 25 °C.

The dioxygen consumption rate in *photosensitizer/TiO_2/ laccase* system with RuP is 25 µmol/ L/ min and in the presence of 100eq NaF, the comsuption decreases and the rate reaches 20 µmol/ L/ min. The dioxygen consumption rate with the *photosensitizer/TiO_2/ laccase* system is higher than with the bimolecular system. Therefore, electron transfer between porphyrin and laccase via TiO_2 is faster than that via the bimolecular system. In the case of RuP, the dioxygen consumption rate of the bimolecular system (30 µM:30 µM) is lower than that of the previous bimolecular system we studied.

Dioxygen consumption measurements using porphyrin (4) and (9) as photosensitizer

Dioxygen consumption measurements with the metallated derivatives with zinc of the above photosensitizers were also investigated for comparison. For both porphyrin (4) and (9), samples containing 2.2 μM of photosensitizer and various concentrations of laccase were prepared as shown in **Table 10** and **Table 11**. Absorption of each of them on TiO_2 nanoparticles was successfully achieved. For porphyrin (4), the amount of photosensitizer attached on TiO_2 nanoparticles was approximately 50% of the initial amount. In contrast, all the amount of porphyrin (9) was successfully absorbed on TiO_2 nanoparticles.

Unfortunately, no dioxygen consumption was observed in any case (**Table 12 and Table 13**). A plausible explanation for this behavior is the formation of aggregates among metallated photosensiter molecules blocking the injection of electrons to the TiO_2 conduction band. However, the exact mechanism needs to be investigated further.

Laccase	Photosensitizer	Consumption (μmol O_2 / L / min)
334 nM	4.4 μM	-
167 nM	2.2 μM	-
167 nM	1.1 μM	-
-	2.2 μM	-

Table 12: Dioxygen consumption results in system photosensitizer/TiO2/ laccase using porphyrin (4) during 2 min irradiation in TEOA buffer (25 mM, 1.5 mL) at pH 6 and 25 ^{o}C.

Laccase	Photosensitizer	Consumption (μmol O_2 / L / min)
167nM	2.2 μM	-
167 nM	1.1 μM	-
16.7 nM	2.2 μM	-
-	2.2 μM	-

Table 13: Dioxygen consumption results in system photosensitizer/TiO2/ laccase using porphyrin (9) during 2 min irradiation in TEOA buffer (25 mM, 1.5 mL) at pH 6 and 25 ^{o}C.

Dioxygen consumption measurements using porphyrin (12) and (13) as photosensitizer

Considering the fact that the system porphyrin (4)/TiO_2/laccase did not consume, we synthesized the porphyrin (12) and its metallated derivative, porphyrin (13) with zinc which bearing alkyl chains between the phenyl groups of the *meso* positions of macroycle ring and the carboxylic anchoring groups. It is known from bibliography that this porphyrin prevent the formation of aggregates. Samples containing photosensitizer/TiO_2/laccase were prepared using porphyrin (12) and porphyrin (13) as photosensitizer. The concentration ratios of photosensitizer and laccase are shown in **Tables (14)** and **(15)**. Unfortunately, none of the two systems did perform any dioxygen consumption.

Laccase	Photosensitizer	Consumption (µmol O_2 / L / min)
167 nM	2.2 µM	-
167 nM	1.1 µM	-
-	2.2 µM	-

Table 14: Dioxygen consumption results in system photosensitizer/TiO_2/ laccase using porphyrin (12) during 2 min irradiation in TEOA buffer (25 mM, 1.5 mL) at pH 6 and 25 ^{o}C.

Laccase	Photosensitizer	Consumption (µmol O_2 / L / min)
167nM	2.2 µM	-
167 nM	1.1 µM	-
-	2.2 µM	-

Table 15: Dioxygen consumption results in system photosensitizer/TiO_2/ laccase using porphyrin (13) during 2 min irradiation in TEOA buffer (25 mM, 1.5 mL) at pH 6 and 25 ^{o}C.

Apart from porphyrins, another group of porphyrinoids are corroles which are similar to porphyrins. They exhibit unique physico-chemical properties due to the direct pyrrole–pyrrole linkage at corrin ring. Corroles [42-44] and their metal complexes have been extensively utilized in the areas of catalysis, sensors, artificial light-harvesting antennas and dye sensitized solar cells. Two substituted corroles bearing carboxylic anchoring groups were also used in this study. Results are the following.

Dioxygen consumption measurements using corrole (14) and (15) as photosensitizer

Samples containing photosensitizer/TiO_2/laccase were prepared using corrole (14) and (15) (**Table 16** and **17**) and the dioxygen consumption for each system was measured. Even though both corroles were successfully attached to TiO_2 - approximately 50% of the initial amount was absorbed on TiO_2 – no dioxygen consumption was detected in any case.

Laccase	Photosensitizer	Consumption (µmol O_2 / L / min)
167 nM	2.2 µM	-
167 nM	1.1 µM	-
-	2.2 µM	-

Table 16: Dioxygen consumption results in system photosensitizer/TiO_2/ laccase using corrole (14) during 2 min irradiation in TEOA buffer (25 mM, 1.5 mL) at pH 6 and 25 ^{o}C.

Laccase	Photosensitizer	Consumption (µmol O_2 / L / min)
167 nM	2.2 µM	-
167 nM	1.1 µM	-
-	2.2 µM	-

Table 17: Dioxygen consumption results in system photosensitizer/TiO_2/ laccase using corrole (15) during 2 min irradiation in TEOA buffer (25 mM, 1.5 mL) at pH 6 and 25 ^{o}C.

Photocatalysis Measurements

Photocatalysis experiments were performed with photosensitizer/TiO_2/laccase systems using porphyrin (2), (4) and RuP since those systems are the only ones that can reduce dioxyen into water as it was proved. We chose the ratios which showed the best results i.e 167 nM of laccase and 2.2 μM of photosensitizer. Unfortunately, we could not achieve the photooxidation of the substrate. A plausible explanation for this behavior is that the photosensitizer was damaged after so many hours of irradiation so the system loses its photocatalytic activity. However, further experiments and studies should be followed in order to make some adjustments and find the appropriate conditions for an efficient system.

Chapter 4

Conclusions

In conclusion, in the first part of this study a laccase from the fungus *Trametes* and various photosensitizers attached to TiO_2 nanoparticles have been investigated for their ability to function in visible-light driven dioxygen reduction. Among the photosensitizers that we studied, only three of them porphyrin (2), porphyrin (7) and RuP showed efficient visible-light-driven conversion. All of them can be successfully absorbed on TiO_2 surface in part with the exception of porphyrin (7) which is totally bound on TiO_2. This behavior could justify the highest dioxygen consumption rate among all systems. Moreover, we determined the best ratios of photosensitizer and laccase leading to optimal performance for each system. In systems where the metallated derivatives of photosensitizers were used no dioxygen reduction was detected. Comparing to the bimolecular system, the presence of TiO_2 enhance the behavior of our systems since the dioxygen consumption rate is much higher.

In the second part, we described the photo-oxidation of p-styrene coupled to the visible-light driven reduction of O_2 by photosensitizer/TiO_2/laccase system in water, at room temperature. We performed the experiments as it is described above, using as photosensitizers porphyrins (2), (4) and RuP complex since those showed the best performance during dioxygen consumption measurement. However, the photosensitizers are getting damaged after so many hours of irradiation, so the system loses its photocatalytic activity and the oxidized products are not detected.

Bibliography

1. Goldet, G., et al., *Electrochemical Kinetic Investigations of the Reactions of [FeFe]-Hydrogenases with Carbon Monoxide and Oxygen: Comparing the Importance of Gas Tunnels and Active-Site Electronic/Redox Effects.* Journal of the American Chemical Society, 2009. **131**(41): p. 14979-14989.
2. Woolerton, T.W., et al., *Efficient and Clean Photoreduction of CO2 to CO by Enzyme-Modified TiO2 Nanoparticles Using Visible Light.* Journal of the American Chemical Society, 2010. **132**(7): p. 2132-+.
3. Reisner, E., et al., *Visible light-driven H(2) production by hydrogenases attached to dye-sensitized TiO(2) nanoparticles.* Journal of the American Chemical Society, 2009. **131**(51): p. 18457-66.
4. Lazarides, T., et al., *Visible Light-Driven O-2 Reduction by a Porphyrin-Laccase System.* Journal of the American Chemical Society, 2013. **135**(8): p. 3095-3103.
5. Schneider, L., et al., *Visible-Light-Driven Oxidation of Organic Substrates with Dioxygen Mediated by a [Ru(bpy)3](2+) /Laccase System.* Chemsuschem, 2015. **8**(18): p. 3048-51.
6. Thurston, C.F., *The Structure and Function of Fungal Laccases.* Microbiology-Sgm, 1994. **140**: p. 19-26.
7. d'Acunzo, F., C. Galli, and B. Masci, *Oxidation of phenols by laccase and laccase-mediator systems - Solubility and steric issues.* European Journal of Biochemistry, 2002. **269**(21): p. 5330-5335.
8. Gavezzotti, P., et al., *Synthesis of Enantiomerically Enriched Dimers of Vinylphenols by Tandem Action of Laccases and Lipases.* Advanced Synthesis & Catalysis, 2011. **353**(13): p. 2421-2430.
9. Giardina, P., et al., *Laccases: a never-ending story.* Cell Mol Life Sci, 2010. **67**(3): p. 369-85.
10. Morozova, O.V., et al., *"Blue" laccases.* Biochemistry (Mosc), 2007. **72**(10): p. 1136-50.
11. Solomon, E.I., *O2 and N2O activation by binuclear, trinuclear, and tetranuclear copper clusters.* Abstracts of Papers of the American Chemical Society, 2007. **233**: p. 138-138.
12. Bento, I., et al., *Dioxygen reduction by multi-copper oxidases; a structural perspective.* Dalton Transactions, 2005(21): p. 3507-3513.
13. Morozova, V., et al., *"Blue" laccases.* Biochemistry-Moscow, 2007. **72**(10): p. 1136-1150.
14. Giardina, P., et al., *Laccases: a never-ending story.* Cellular and Molecular Life Sciences, 2010. **67**(3): p. 369-385.
15. Bento, I., M.A. Carrondo, and P.F. Lindley, *Reduction of dioxygen by enzymes containing copper.* Journal of Biological Inorganic Chemistry, 2006. **11**(5): p. 539-47.
16. Bento, I., et al., *Mechanisms underlying dioxygen reduction in laccases. Structural and modelling studies focusing on proton transfer.* Bmc Structural Biology, 2010. **10**.
17. Lee, S.K., et al., *Nature of the intermediate formed in the reduction of O(2) to H(2)O at the trinuclear copper cluster active site in native laccase.* Journal of the American Chemical Society, 2002. **124**(21): p. 6180-93.

18. Quintanar, L., et al., *Role of aspartate 94 in the decay of the peroxide intermediate in the multicopper oxidase Fet3p.* Biochemistry, 2005. **44**(16): p. 6081-91.
19. Bento, I., et al., *Dioxygen reduction by multi-copper oxidases; a structural perspective.* Dalton Trans, 2005(21): p. 3507-13.
20. Madhavi, V. and S.S. Lele, *Laccase: Properties and Applications.* Bioresources, 2009. **4**(4): p. 1694-1717.
21. Reinhamm.Br, *Oxidation-Reduction Potentials of Electron Acceptors in Laccases and Stellacyanin.* Biochim Biophys Acta, 1972. **275**(2): p. 245-&.
22. Shleev, S., et al., *Direct electron transfer between copper-containing proteins and electrodes.* Biosensors & Bioelectronics, 2005. **20**(12): p. 2517-2554.
23. Shleev, S., et al., *Characterization of two new multiforms of Trametes pubescens laccase.* Bioorganic Chemistry, 2007. **35**(1): p. 35-49.
24. Eggert, C., et al., *Molecular analysis of a laccase gene from the white rot fungus Pycnoporus cinnabarinus.* Appl Environ Microbiol, 1998. **64**(5): p. 1766-72.
25. Piontek, K., M. Antorini, and T. Choinowski, *Crystal structure of a laccase from the fungus Trametes versicolor at 1.90-A resolution containing a full complement of coppers.* Journal of Biological Chemistry, 2002. **277**(40): p. 37663-9.
26. Omura, T., *Studies on laccases of lacquer trees. I. Comparison of laccases obtained from Rhus vernicifera and Rhus succedanea.* Journal of Biochemistry, 1961. **50**: p. 264-72.
27. Claus, H., *Laccases: structure, reactions, distribution.* Micron, 2004. **35**(1-2): p. 93-96.
28. Dolphin, D., *"The Porphyrins".* Academic Press, 1978. **Vol. 1**.
29. *"Porphyrins and Metalloporphyrins",.* Elsevier Scientific Publishing Company, 1975: p. 2-28.
30. Battersby, A.R., Nat. Prod. Rep, 2000. **17**: p. 507

31. R. Lemberg, J.W.L., Hematin Compounds and Bile Pigments, Interscience, 1949.
32. Ashford, D.L., et al., *Molecular Chromophore-Catalyst Assemblies for Solar Fuel Applications.* Chem Rev, 2015.
33. Kostas, I.D., et al., *The first use of porphyrins as catalysts in cross-coupling reactions: a water-soluble palladium complex with a porphyrin ligand as an efficient catalyst precursor for the Suzuki–Miyaura reaction in aqueous media under aerobic conditions.* Tetrahedron Letters, 2007. **48**(38): p. 6688-6691.
34. D. E. Tronrud, M.F.S., B. W. Matthews, J. Mol. Biol, 1986. **188**: p. 443.
35. E. Gudowska-Novak, M.D.N., J. Fajer, J. Phys. Chem, 1990. **94**: p. 5795.
36. S. M. Prince, M.Z.P., A. A. Freer, G. McDermott, A. M. Hawthornwaite-Lawless, R. J. Cogdell, N. W. Isaacs, J. Mol. Biol, 1997. **268**: p. 412.
37. Kadish, K.M., K.M. Smith, and R. Guilard, *The porphyrin handbook*2000, San Diego: Academic Press.
38. Ladomenou, K., et al., *The importance of various anchoring groups attached on porphyrins as potential dyes for DSSC applications.* Rsc Advances, 2014. **4**(41): p. 21379-21404.

39. Schneider, L., et al., *Visible-Light-Driven Oxidation of Organic Substrates with Dioxygen Mediated by a [Ru(bpy)(3)](2+)/Laccase System.* Chemsuschem, 2015. **8**(18): p. 3048-3051.
40. Zeitler, K., *Photoredox catalysis with visible light.* Angew Chem Int Ed Engl, 2009. **48**(52): p. 9785-9.
41. Stangel, C., et al., *Noble metal porphyrin derivatives bearing carboxylic groups: Synthesis, characterization and photophysical study.* Polyhedron, 2013. **52**: p. 1016-1023.
42. Ding, T., et al., *Photophysical properties of a series of free-base corroles.* Journal of Physical Chemistry A, 2005. **109**(33): p. 7411-7417.
43. Barbe, J.M., et al., *Synthesis and physicochemical characterization of meso-functionalized corroles: Precursors of organic-inorganic hybrid materials.* European Journal of Organic Chemistry, 2005(21): p. 4601-4611.
44. Grigg, R., et al., *Spectroscopic Study of Protonation of Porphins and Corroles.* Journal of the Chemical Society-Perkin Transactions 2, 1973(4): p. 407-413.